Intrinsic Rotation Regimes in TCV L-mode Plasmas

A.Bortolon, B.P.Duval, Y. Andrebe, A. Karpushov and the TCV team.

Centre de Recherche en Physique des Plasmas, EPFL
Association EURATOM

Introduction and Motivation

- Plasma rotation has a role in many aspects of confined plasmas performances (energy confinement, transport barriers, RWM stabilization)

- Need for reliable models to predict intrinsic rotation in large fusion devices

- Robust experimental observations in H-mode from different machines: co current toroidal rotation, scaling with plasma energy

- L-mode shows more rich phenomenology: useful to assess interplay between different aspects

  - Neoclassical rotation
  - Turbulent momentum transport
  - MHD effect
  - Coupling core–edge physics

CXRS diagnostic in TCV

CXRS diagnostic is composed of 3 systems optimized for observation of the Carbon VI 529.1 nm CX emission from Diagnostic Neutral Beam Injector

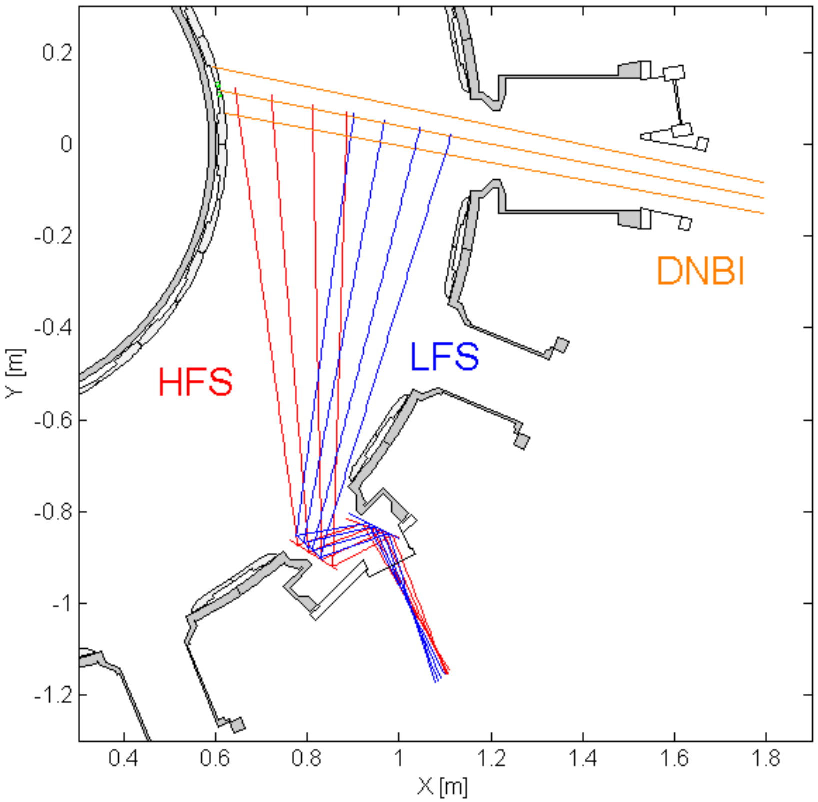

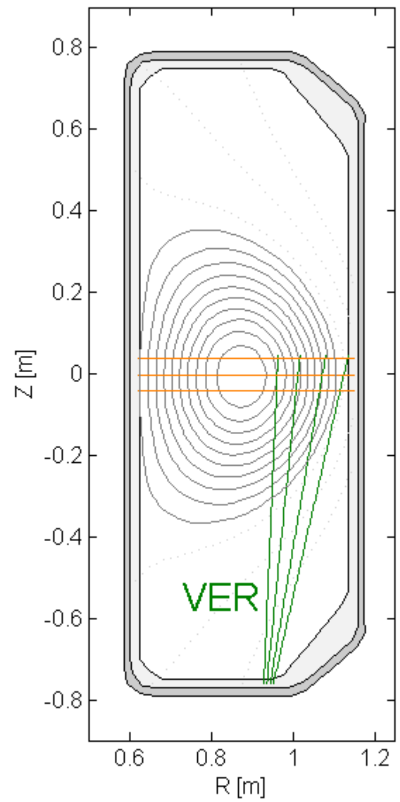

Diagnostic Neutral Beam Injector (H^0)

- Injection angle 11°
- Extracted current 3A, acceleration voltage 50 kV
- Injected power < 80 kW
- 20-70% absorption (mainly on the electrons)
- 50-100 ms modulation for background subtraction

Negligeable applied torque

CXRS upgrade

During TCV opening (2007-2008) CXRS diagnostic has been upgraded in both **observation configuration** and **detection system**

Each system is now equipped with:

1. **2 bundles of 20 optic fibers**
   40 chords in *coupled* or *extended* configuration
2. **Czerny-Turner spectrometer**
   1. f/7.5, 2400l/mm holographic grating
   2. double entrance slit
   3. optical reducer/intensifier
3. **CCD back illuminated detector**
   512x512 pixels, frame transfer, double node read out

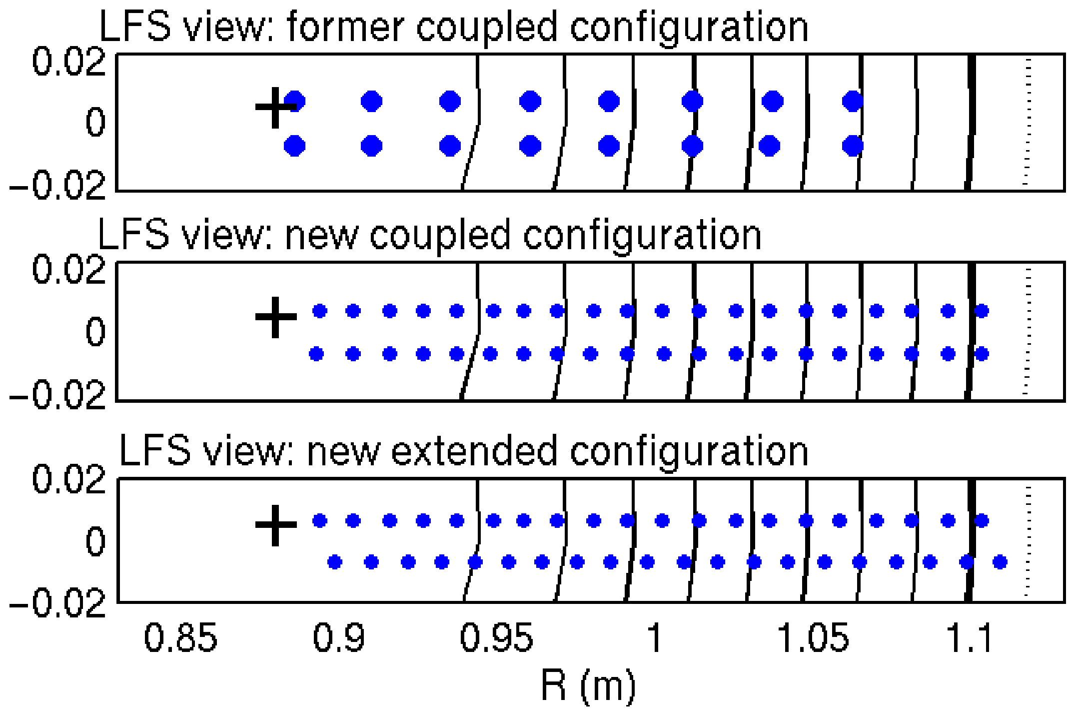

Higher radial resolution (2.5→1 cm)

Radial coverage up to plasma edge

Summary

1. Limited L-mode
   – Co and counter current toroidal rotation regimes
   – Triangularity effect
   – Radial electric field

2. Diverted L-mode
   – Co and counter current toroidal rotation regimes
   – Magnetic configuration effect
   – Radial electric field

3. Momentum transport estimates

Summary

1. Limited L-mode
   – Co and counter current toroidal rotation regimes
   – Triangularity effect
   – Radial electric field

2. Diverted L-mode
   – Co and counter current toroidal rotation regimes
   – Magnetic configuration effect
   – Radial electric field

3. Momentum transport estimates

Stationary u_φ in limited L-mode

lim

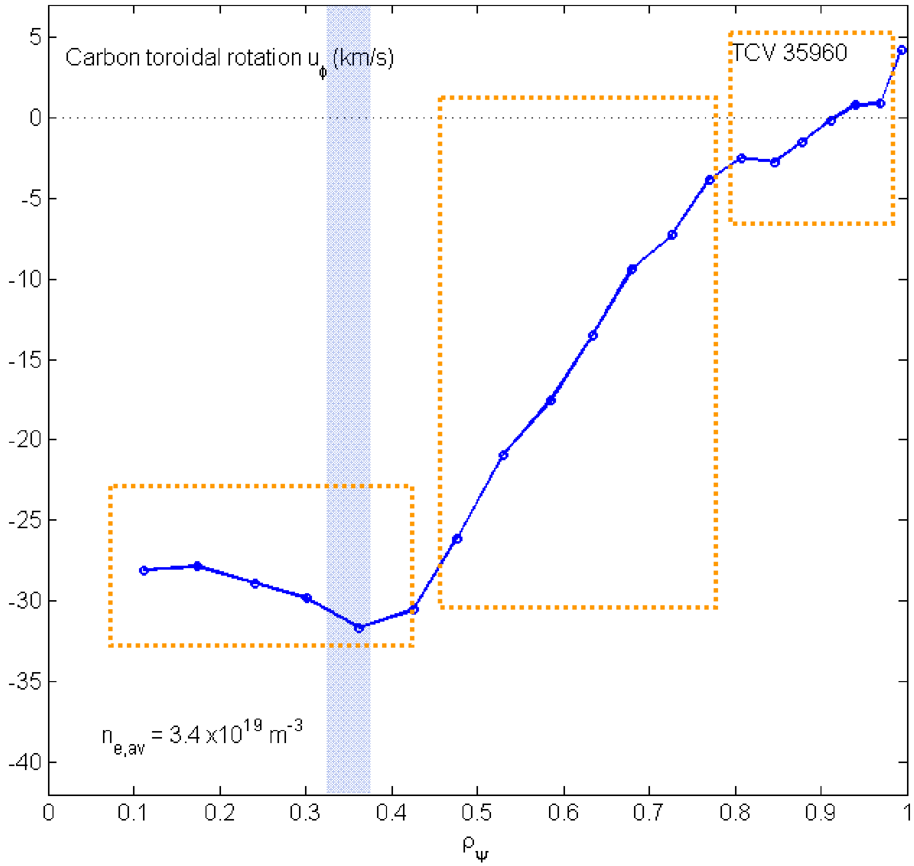

Typically counter current rotation is observed

1. **Core region** ($\rho<\rho_{inv}$): convex $u_\varphi(r)$ due to sawteeth (τ_{ST} ~ 5 ms)
2. **Intermediate region** ($\rho_{inv}<\rho<0.85$): $u_\varphi(\rho) \propto T_i(\rho)$
3. **Edge region** ($\rho>0.85$): $u_\varphi(\rho) \leq 0$

Stationary u_φ in limited L-mode

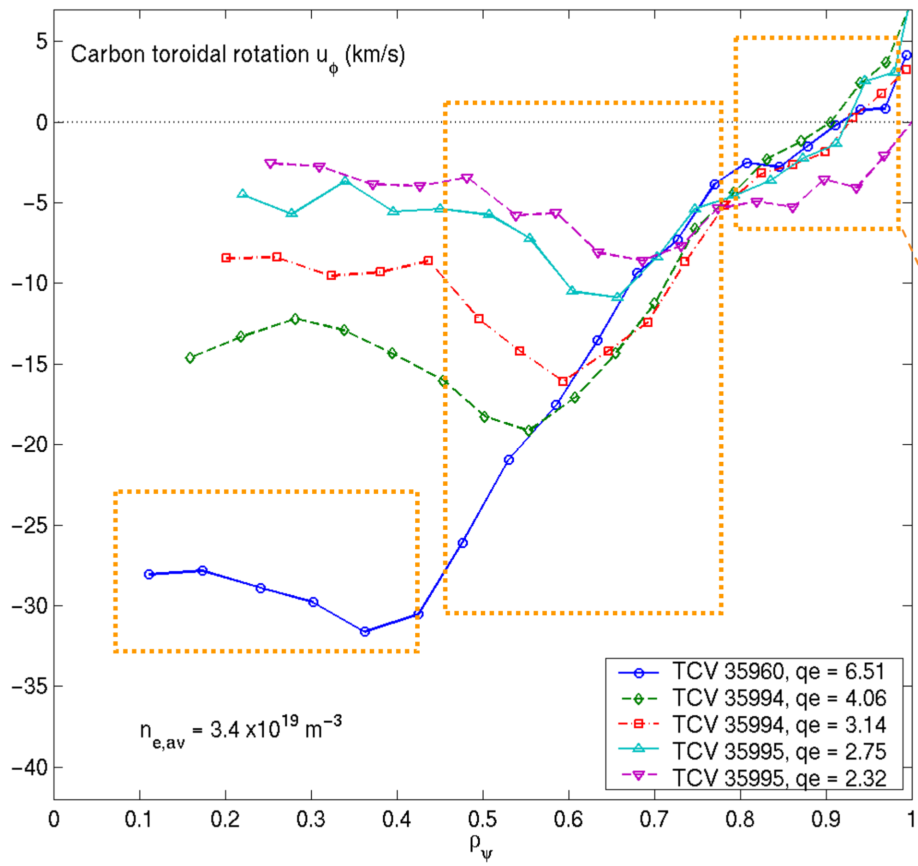

Typically counter current rotation is observed

1. **Core region** ($\rho<\rho_{inv}$): convex $u_\varphi(r)$ due to sawteeth (τ_{ST} ~ 5 ms)
2. **Intermediate region** ($\rho_{inv}<\rho<0.85$): $u_\varphi(\rho) \propto T_i(\rho)$
3. **Edge region** ($\rho>0.85$): $u_\varphi(\rho) \leq 0$

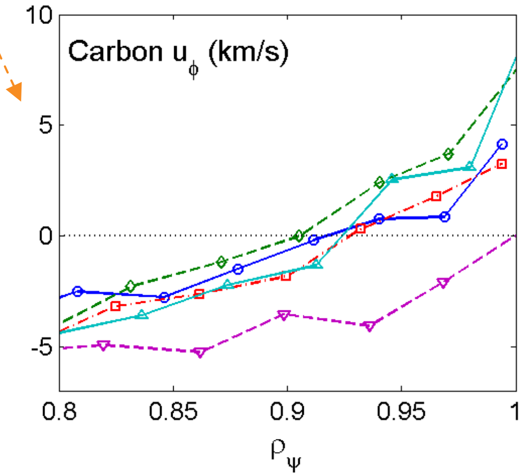

- u_ϕ max determined by sawteeth inversion radius
- At lowest q_e sawtooth affect the gradient region $\rightarrow$ flat u_ϕ profile

Poloidal rotation profile u_θ

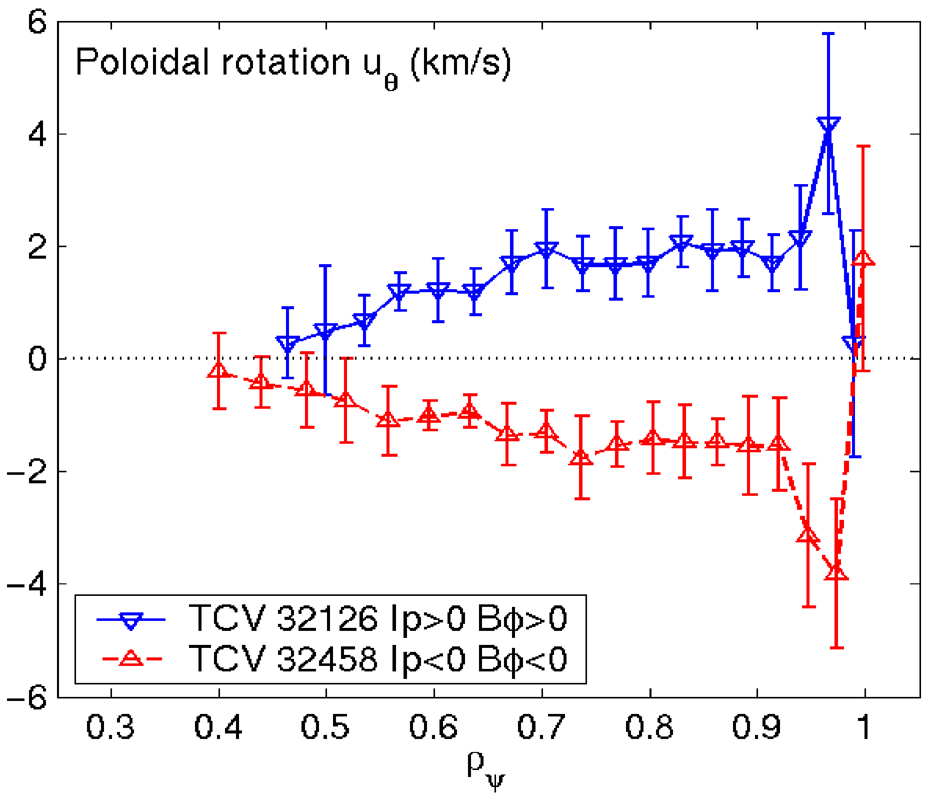

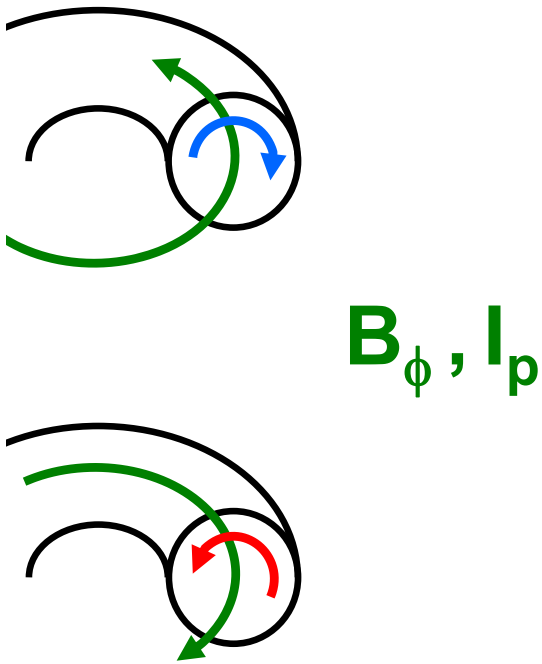

- Profile reverses with B_ϕ reversal
- u_θ ~1-2 km/s, close to neoclassical values (0.05-2 km/s)
- Decreasing towards the core
- Peak close to the edge

Toroidal rotation inversion

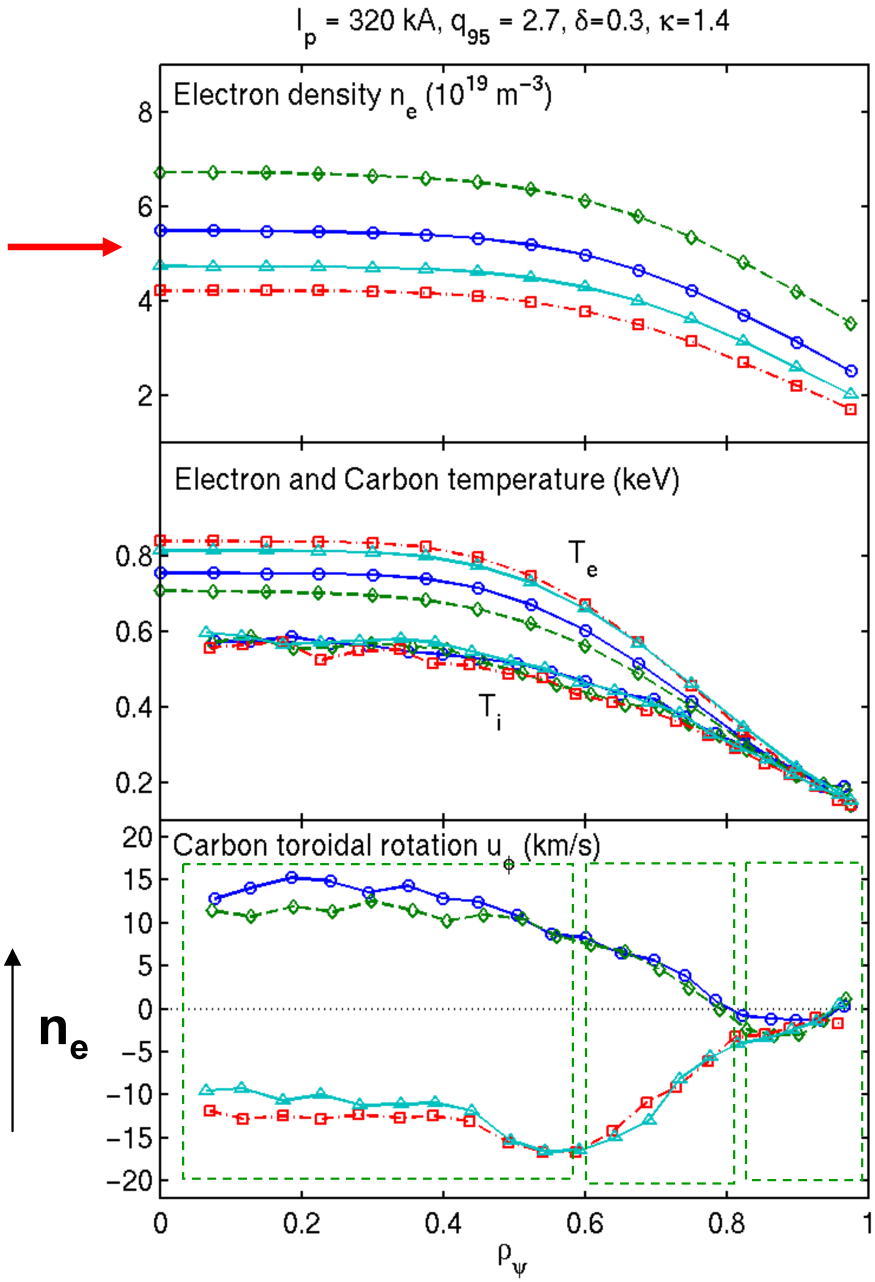

For n_{e0}>4x10^{19} m^{-3} *and* q_e~3
co-current rotation profile

- Similar core velocity $u_{\varphi 0}$~10-15 km/s
- u_φ peaking in the core region (sawtooth effect)
- Reverse gradient in intermediate region
- Similar u_φ(0.85) ~ -3 km/s
- Smooth variation of temperature and density profiles

u_φ profile evolution across inversion

lim

I_p=340 kA, δ=0.3, κ=1.4, B_φ=1.4T

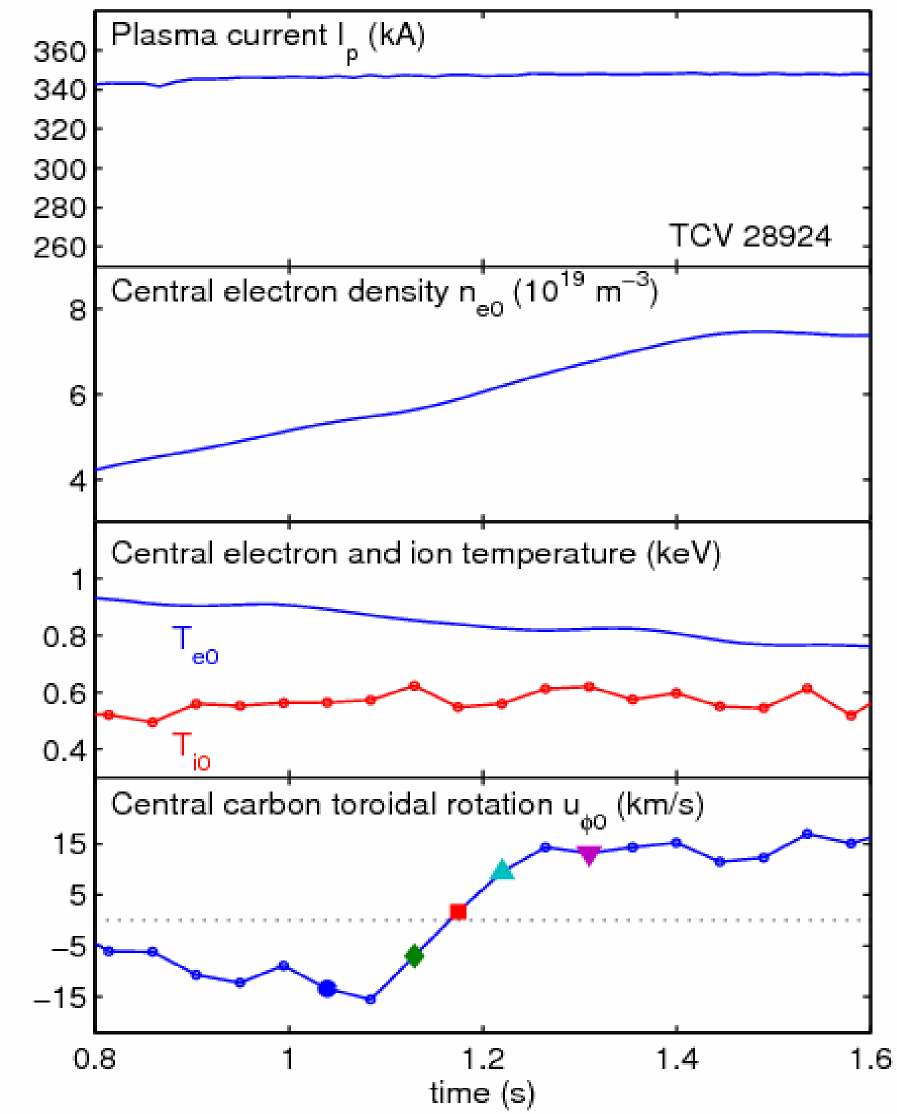

Rotation inversion obtained with a density ramp at I_p=const

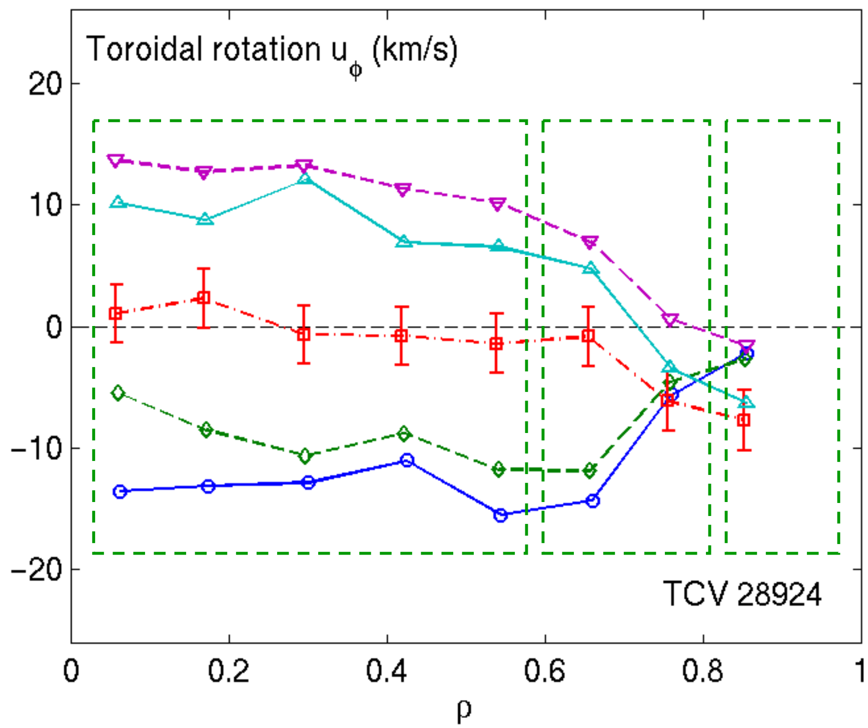

- Core accelerates rigidly
- Transient cnt-acceleration of the edge
- Momentum conservation dynamic followed by edge dissipation

Rotation inversion reproducible

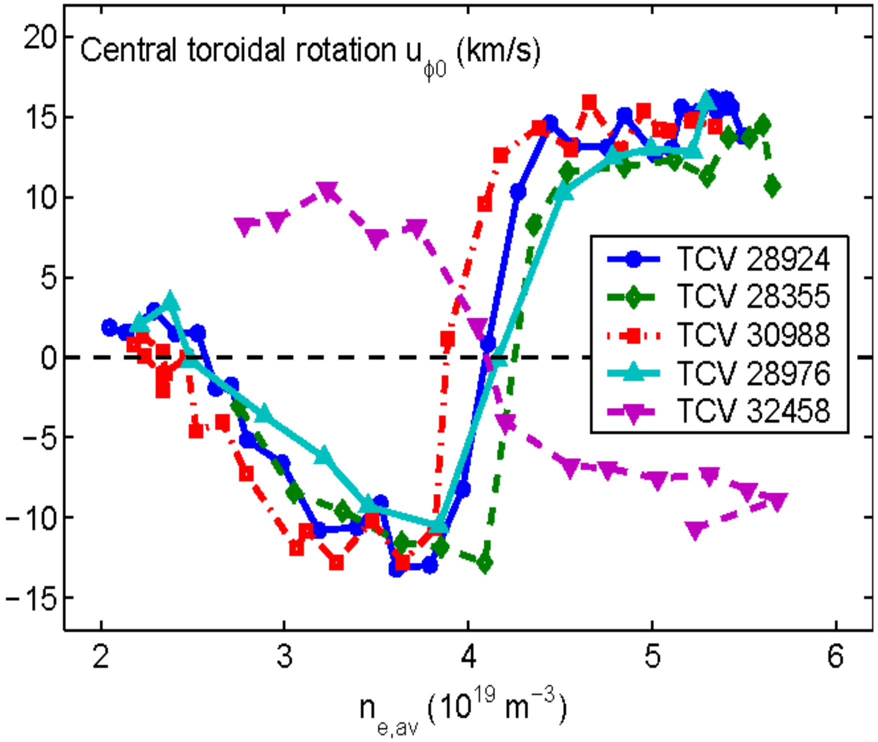

Different density ramp discharges

I_p=340kA, δ=0.3

- Well defined n_e threshold
- Discharges separated by >3000 shots
- TCV 32458 curve corresponding to inversed I_p
- Little effect of machine conditioning (Boronised)
- Physical phenomenon

MHD activity

Mirnov coil spectrogram

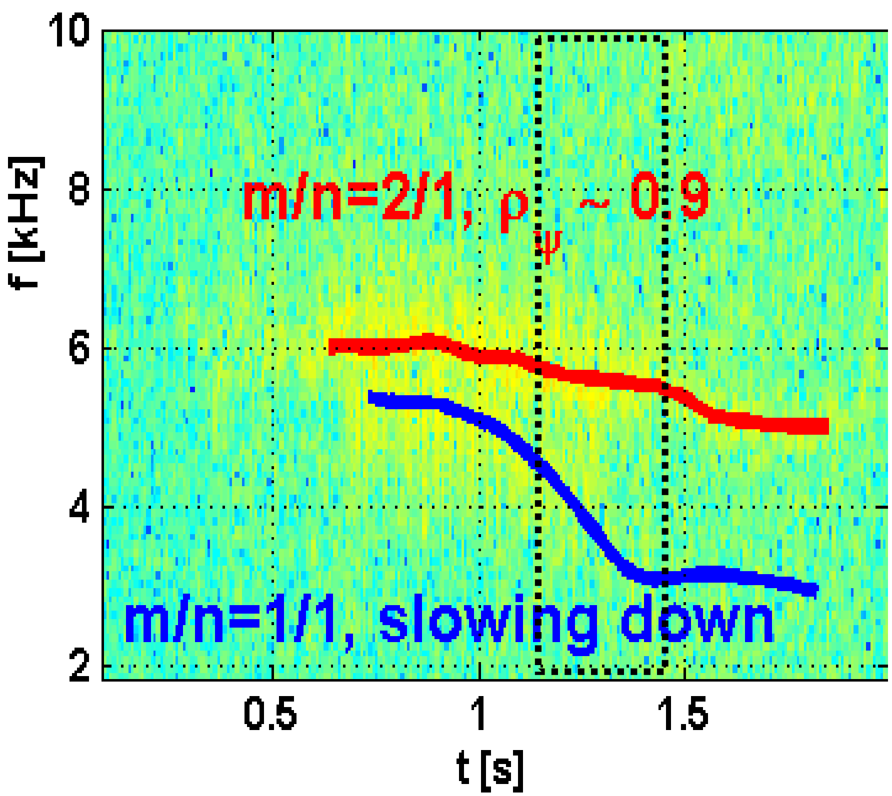

Rotation inversion is often accompanied by MHD activity

- **Small peripheral mode (m=2,n=1) at 6 kHz**
- **Sawtooth crash precursor (1,1) at ρ_{inv}~0.5**

1. Across the inversion precursor frequency slows down (5 to 3 kHz)
2. After inversion precursor is less active (1 oscillation per crash) and the two modes evolve independently

Triangularity scan

q_{95} 2.9 2.5

Density ramps discharges
at constant I_p

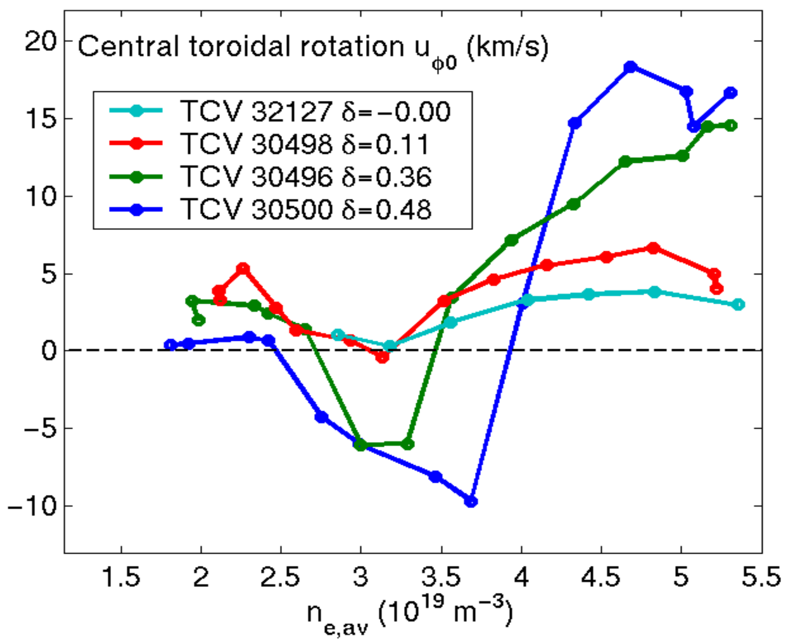

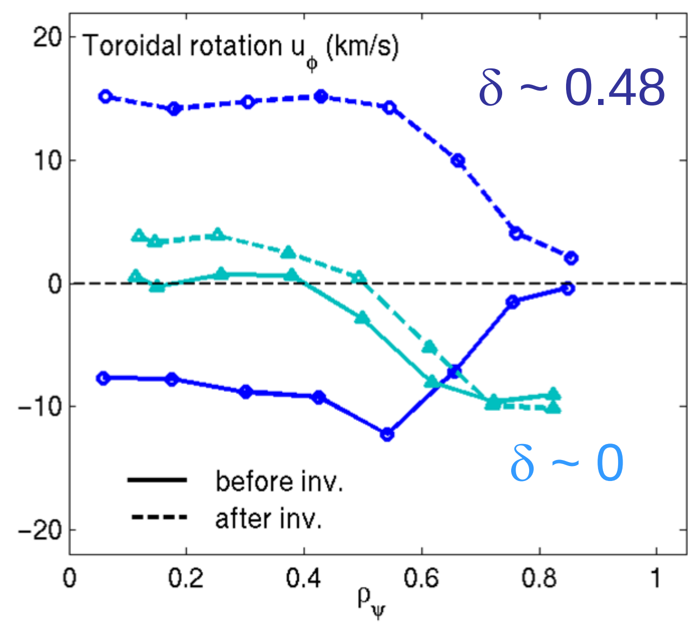

- Inversion diminishes with δ
- Still some change at ~same density
- Plasma edge “spins up”

Poloidal rotation and radial electric field

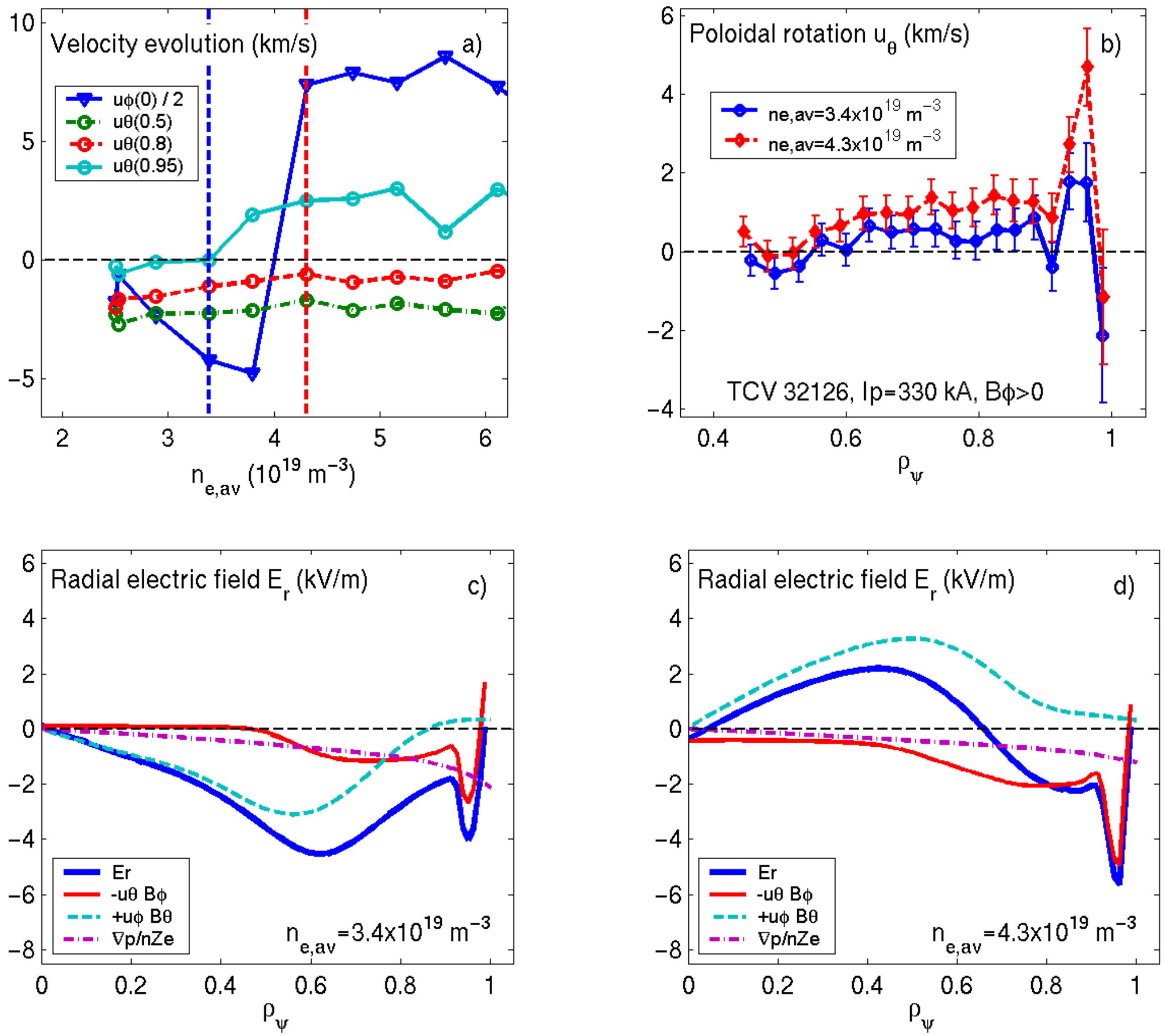

Rotation inversion obtained in density ramp

- Slight increase of u_θ with density
- E_r peaks near the edge (smooth extrapolations to the edge for u_ϕ and ∇p)

Before inversion: E_r<0

After the inversion:

- **E_r<0 in the edge**
- **E_r>0 in the core**

NO ABRUPT CHANGE IN CONFINEMENT OBSERVED

Summary

1. Limited L-mode
   – Co and counter current toroidal rotation regimes
   – Triangularity effect
   – Radial electric field

2. Diverted L-mode
   – Co and counter current toroidal rotation regimes
   – Magnetic configuration effect
   – Radial electric field

3. Momentum transport estimates

Stationary u_φ profile: I_p dependence

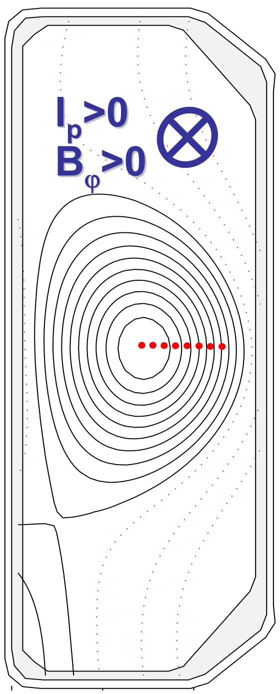

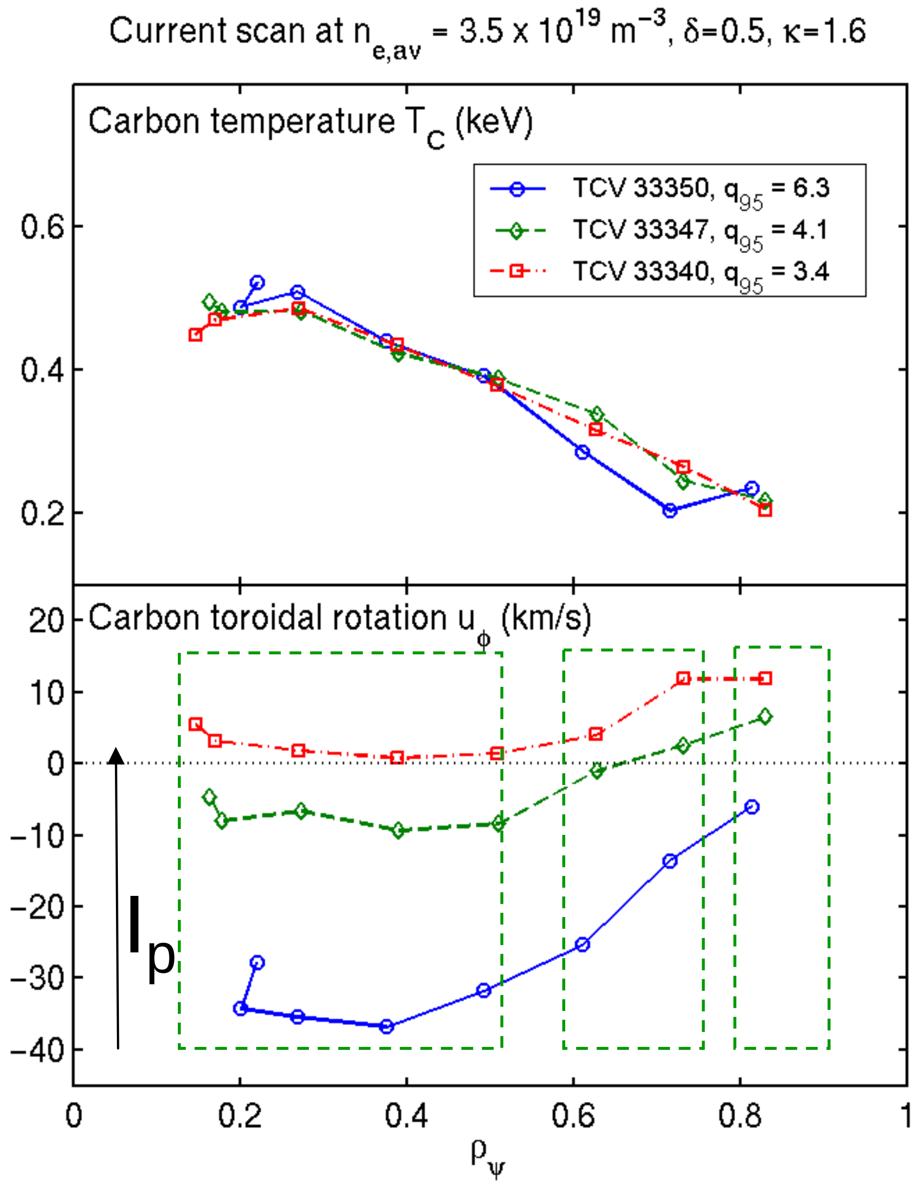

Stationary profile
in shot by shot current scan
Lower Single Null Configuration

- Core flattened by sawtooth
- Edge rotation scales with I_p
- $u_\phi(0.8)$ from co to cnt

∇u_ϕ sign appears independent from u_ϕ values

Stationary u_φ profile: n_e dependence

$I_p>0$, $B_\varphi>0$, LSN, UNFAV

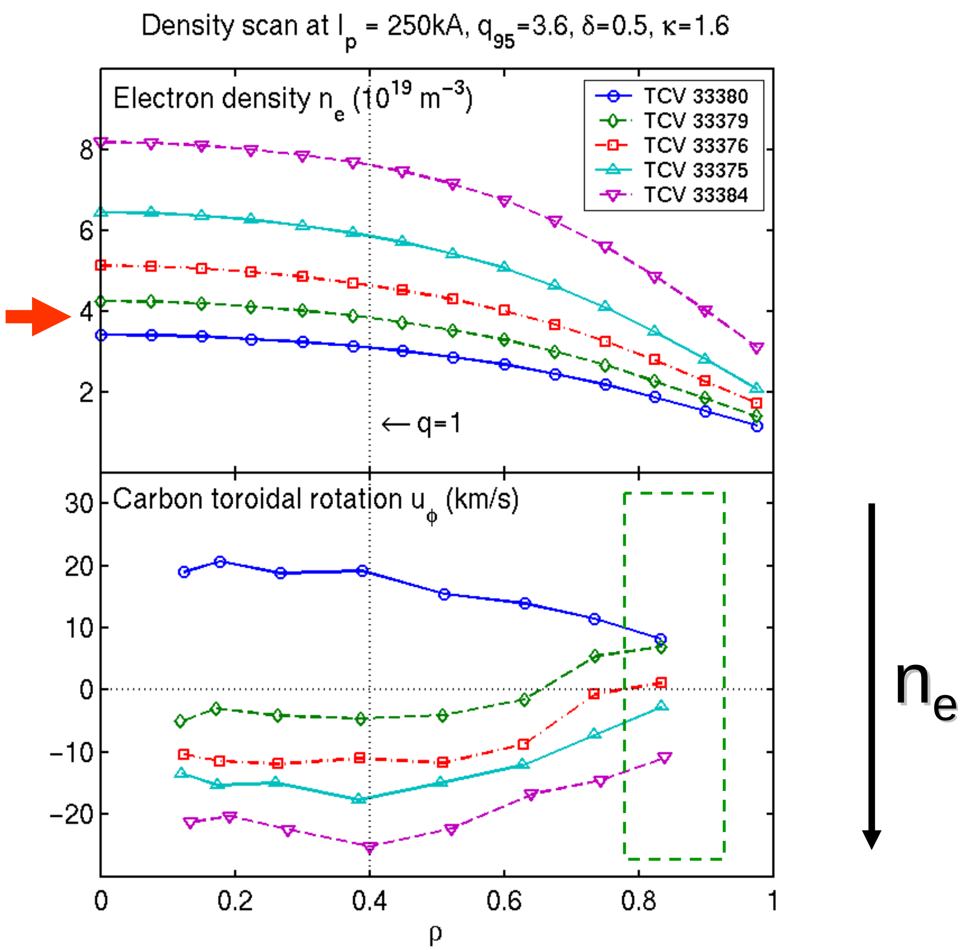

Stationary profile in shot by density scan

Lower Single Null Configuration

2 regimes observed

- $n_{e0}>4\times10^{19}$ m^{-3} hollow profile
- $n_{e0}<4\times10^{19}$ m^{-3} peaked profile

- **Opposite effect respect to limited discharges!**

- Variation of $u_\varphi(0.85)$ with n_e
- Rigid shift of profile with density

Magnetic configuration effect

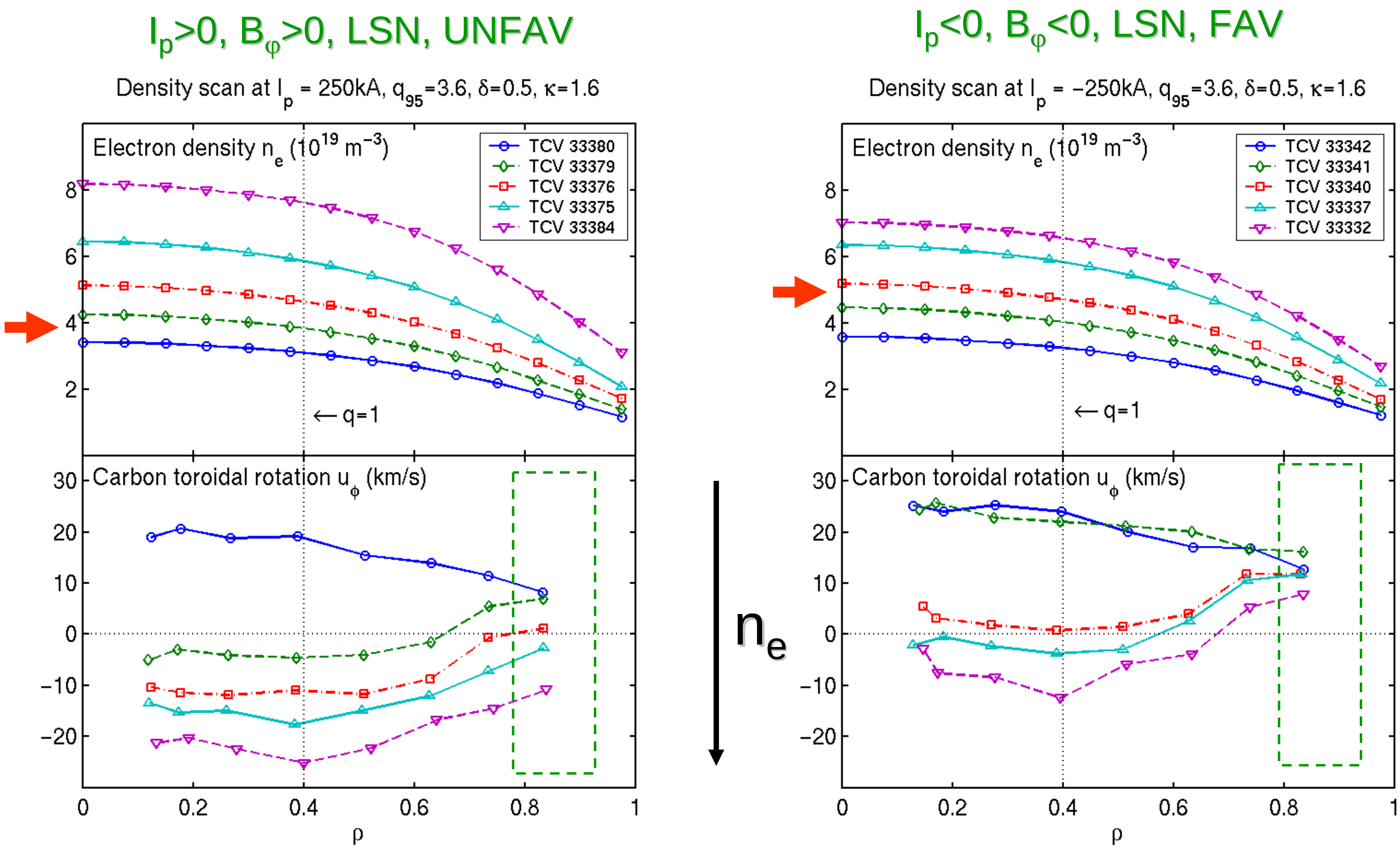

- Rotation profile reverses (but at different densities)
- Different edge behavior for changing ∇B ion drift direction

Edge u_φ dependence on n_e

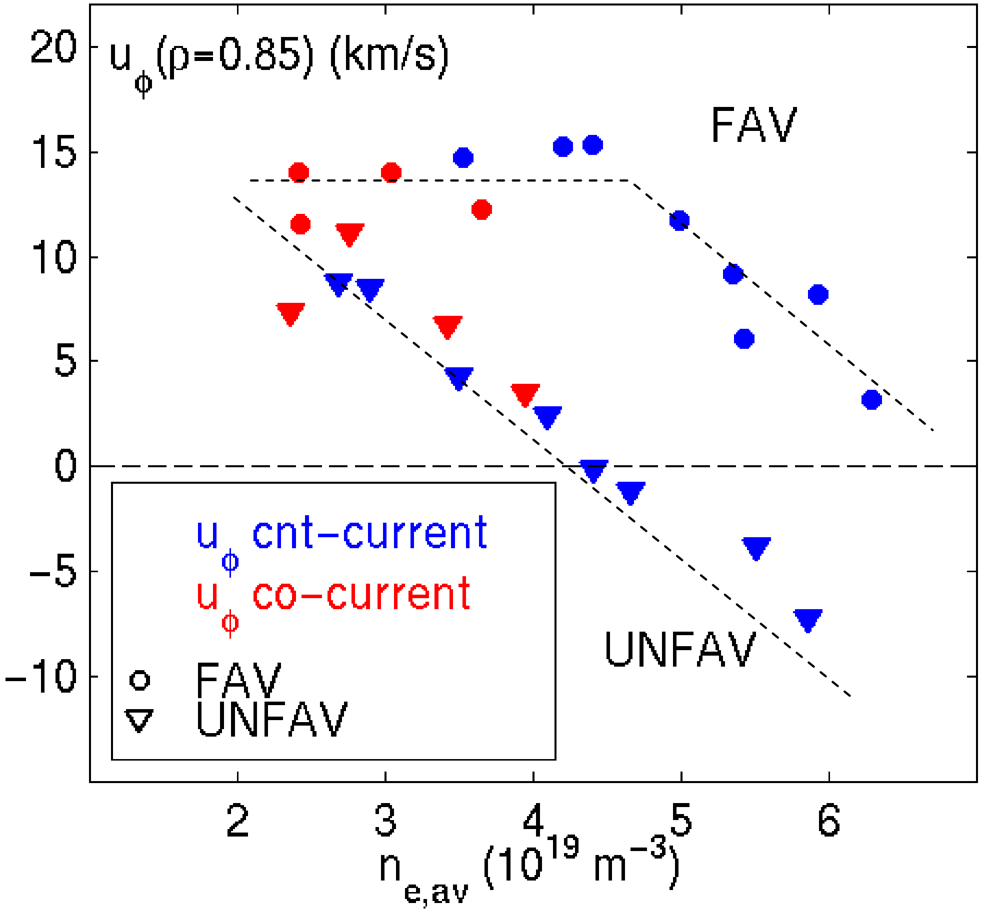

- u_φ(0.85) decreases with n_e
- 10 km/s offset between FAV and UNFAV configurations

Tempting link between measured SOL parallel flows:

- TCV collisional flows measured on LFS decrease with n_e
- transport driven flow induces asymmetry between configurations

u_φ(0.85) independent on the core rotation regime

MHD activity

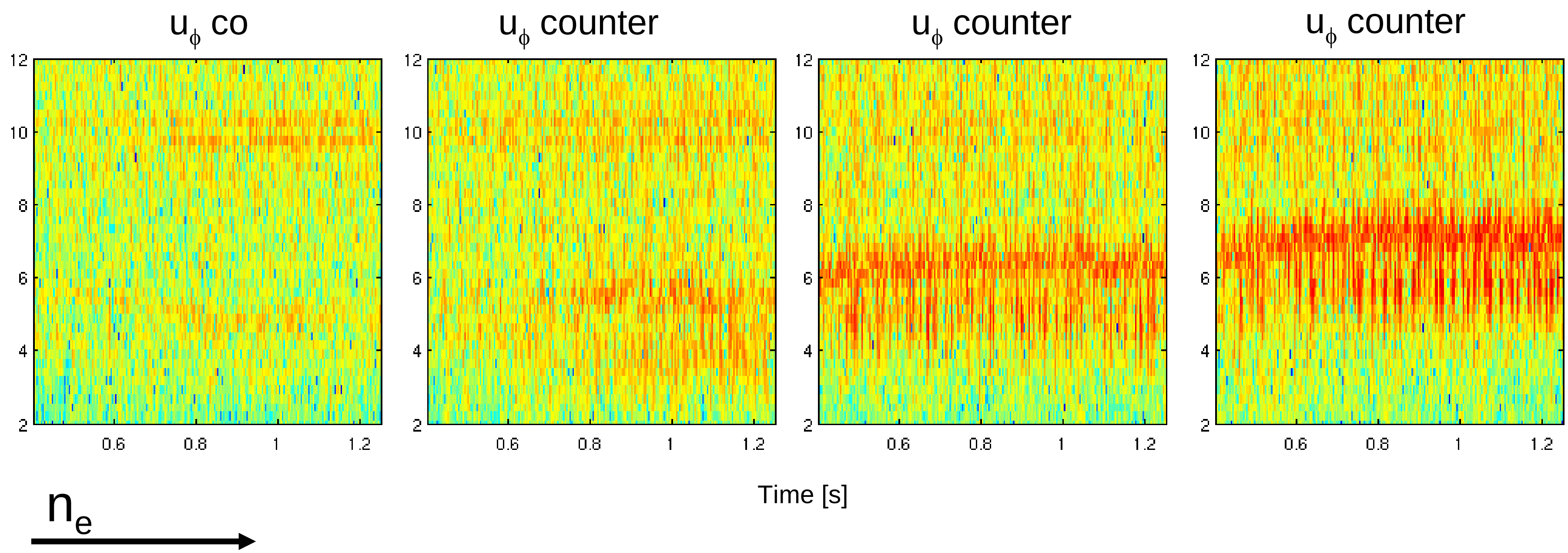

- Sequence of diverted discharges: stationary conditions, density scan
- [2,1] mode, close to plasma periphery
- [1,1] mode (sawteeth precursor)

- Correlation of mode increase frequency with increasing plasma density

Poloidal rotation and radial electric field

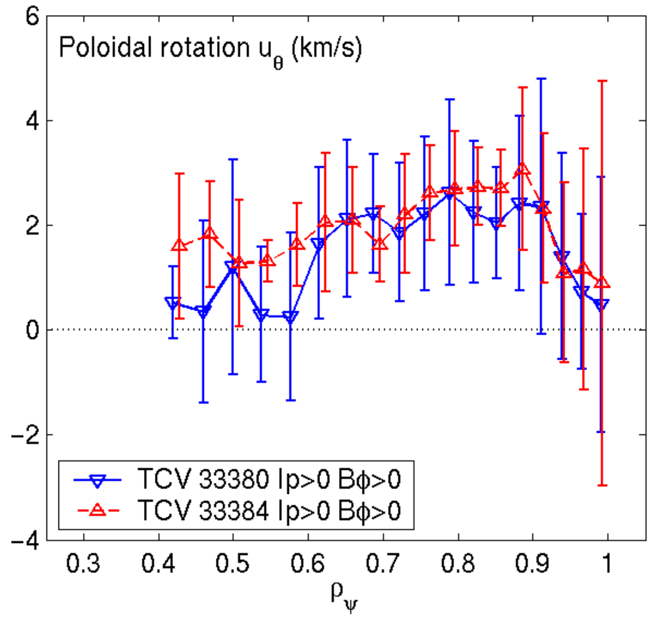

Poloidal rotation profile for 2 discharges at extreme densities (n_e=2.5, 6x10^{19} m^{-3})

- ❖ Little u_θ variation in the uncertainties
- ❖ Smooth decrease to zero at the edge (peak is absent)

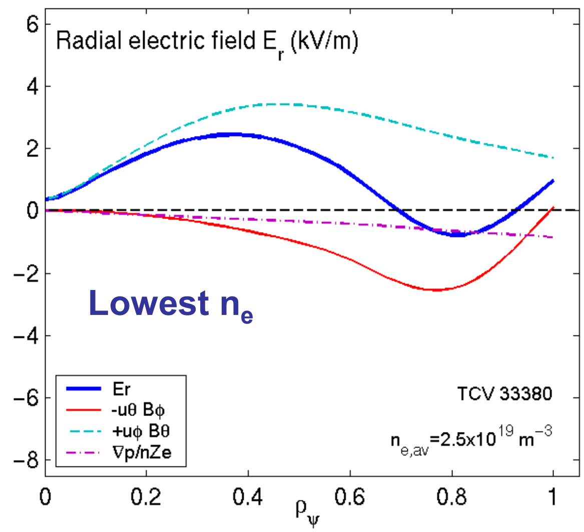

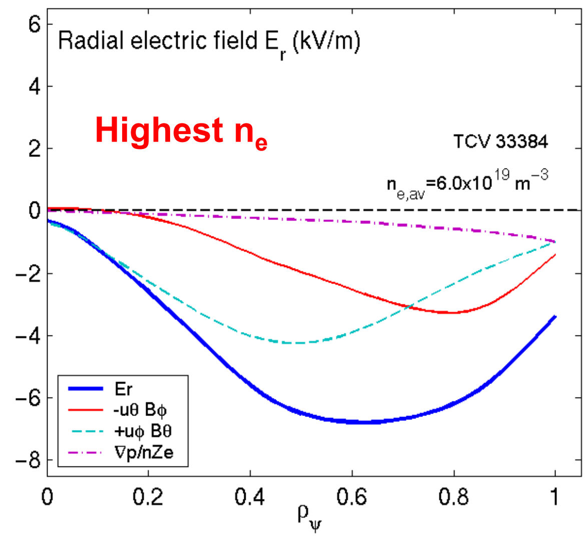

Large difference in E_r

Low n_e:

E_r>0 in the core

High n_e:

E_r<0

NO ABRUPT CHANGE IN CONFINEMENT OBSERVED

Summary

1. Limited L-mode
   - Co and counter current toroidal rotation regimes
   - Triangularity effect
   - Radial electric field

2. Diverted L-mode
   - Co and counter current toroidal rotation regimes
   - Magnetic configuration effect
   - Radial electric field

3. Momentum transport estimates

Momentum transport characterization

In absence of external torque the toroidal velocity profile is determined by:

1. **radial momentum transport** (∇u_ϕ, core physics)
2. **boundary condition** (edge physics)

$$\frac{du_\varphi}{dt} + \nabla \cdot \Gamma = 0$$

$$\Gamma = -D\frac{du_\varphi}{dr} + v_c u_\varphi + \Gamma_{ND}$$

Viscosity

(flattening effect, time scale)

Convective pinch

(builds up a gradient if $u \neq 0$)

Intrinsic torque

may sustain a gradient when u=0, Residual Reynolds stress

- ❖ TCV has no torque direct modulation
- ❖ Transport coefficients estimated in spontaneous transient phases
- ❖ Transport equation solved in 1D cylindrical model for selected cases and combination of transport coefficients

u_φ inversion from intrinsic torque variation

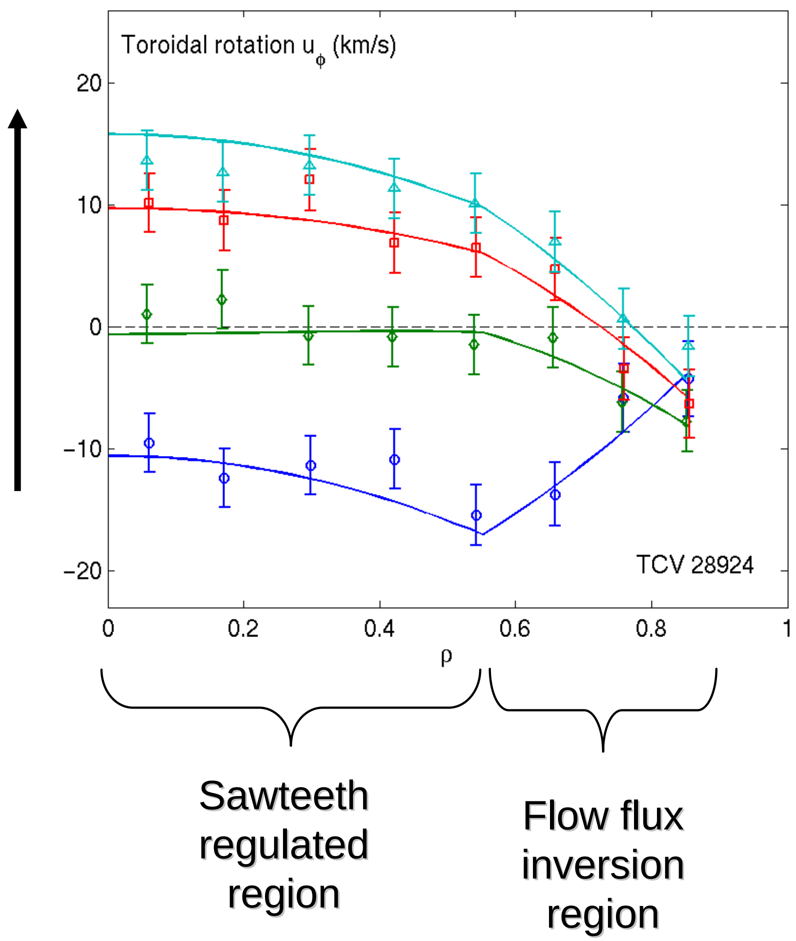

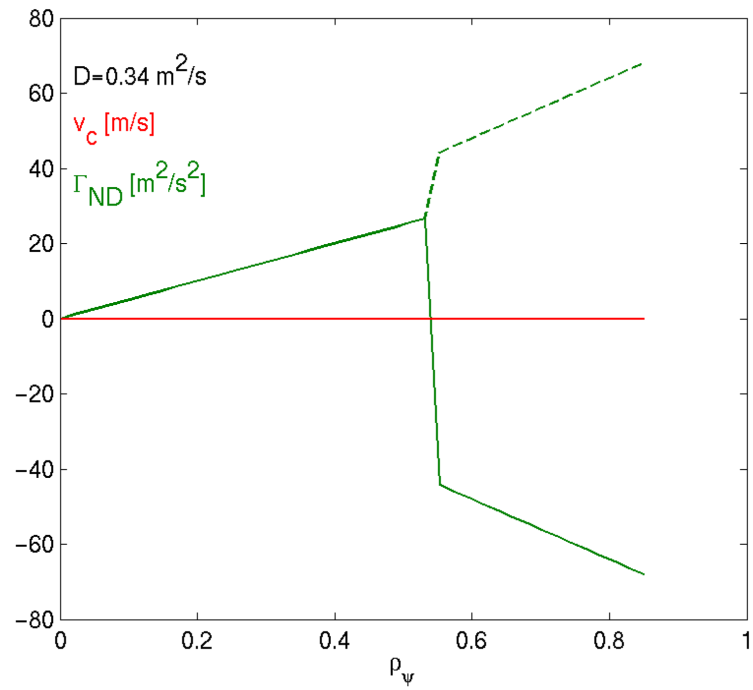

Viscous drag at boundary condition

$\Gamma_{b.c.} = -k\,[\,u_{\varphi,b.c.} - u_{\varphi,stat.}]$

edge dissipation, determining dynamic of the total momentum variation

- **D = 0.34 m^2/s >100 $D_{\varphi,Neo}$**
- **Transient edge acceleration reproduced**
- **Final u_φ profile crossing zero is sustained**

u_φ inversion from convective pinch

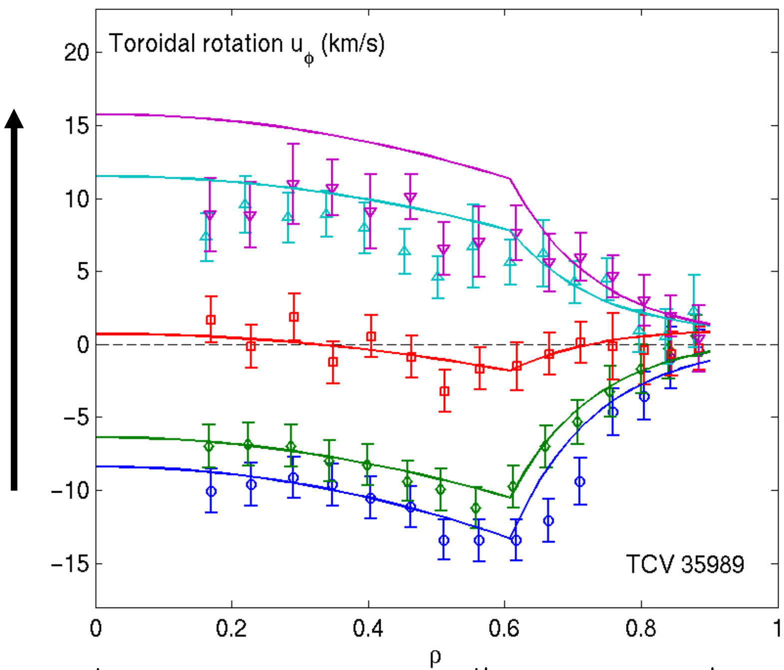

Sawteeth regulated region

Flow flux inversion region

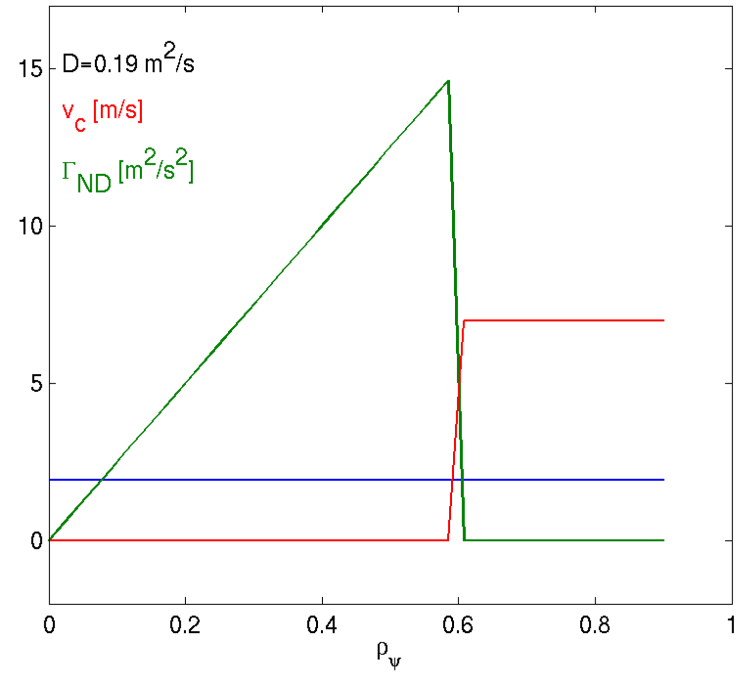

Boundary condition velocity changing sign

$u_{\varphi,b.c.} = -3 \rightarrow +3$ km/s at the inversion determining change of direction of convective momentum flux

- **D = 0.19 m^2/s >100 $D_{\varphi,Neo}$**
- **v_c = 6 m/s**
- **No change in underlying physics is implied**

Conclusions

- Intrinsic rotation observed in Ohmic L-mode
  - Limited L-mode (2 regimes)
    - Low density counter current
    - High density co-current
    - **Edge velocity close to zero positive at LCFS**
  - Diverted L-mode (2 regimes)
    - Low density co-current
    - High density counter current (limited behavior)
    - **Edge velocity varies with current and density and acts as boundary condition**
- Role of MHD in rotation inversion
- Large excursion in u_ϕ and E_r without dramatic change in confinement

Conclusions (2)

3 regions interpretation scheme:

- **Core region: sawteeth**
  - ECH for sawteeth modification to study possible torque co current directed
- **Edge region: physics of boundary condition**
  - effect of plasma shape
  - parallel SOL fluxes, neutrals friction
- **Intermediate region: non diffusive fluxes**
  - which mechanisms can provide the non diffusive fluxes with the required dependencies?

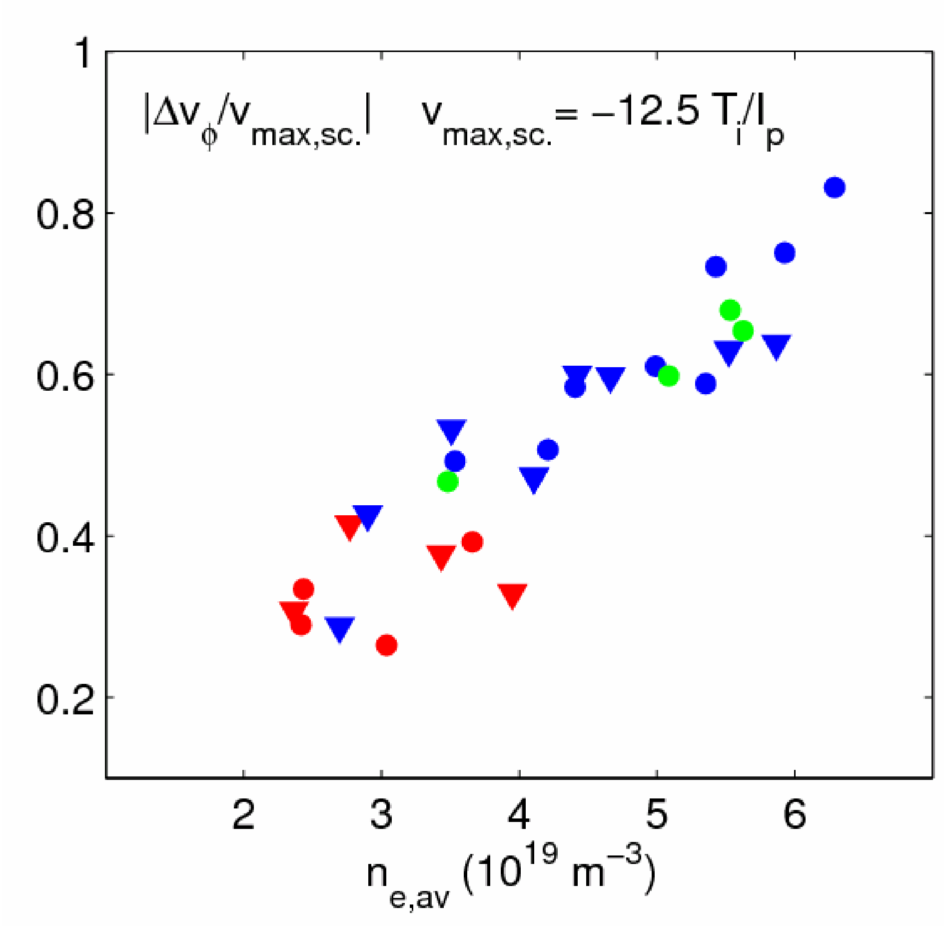
$|\Delta v_\phi / v_{max,sc.}|$
$v_{max,sc.} = -12.5\, T_i/I_p$
1
0.8
0.6
0.4
0.2
2
3
4
5
6
$n_{e,av}$ (10^{19} m^{-3})

Model results: inversion in diverted L-mode

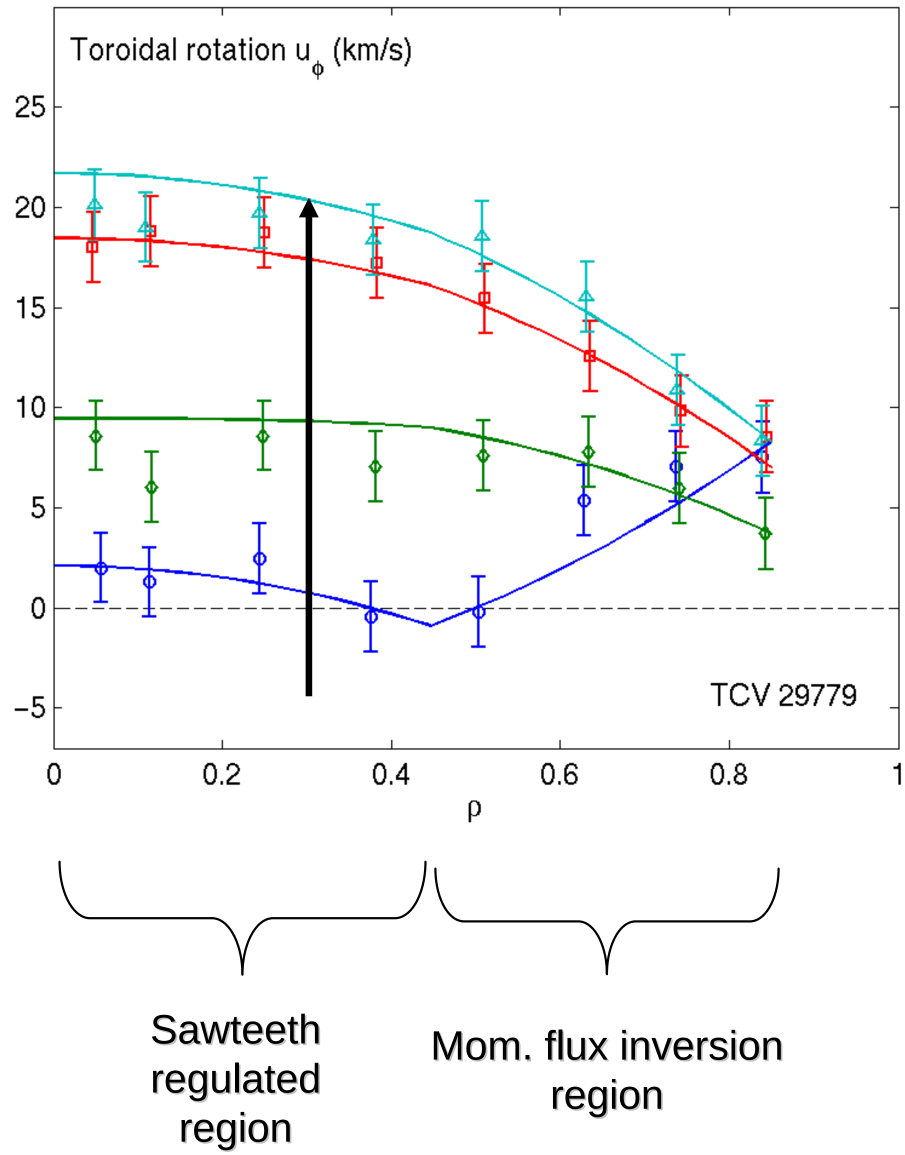

- Reasonably good agreement
- Main features are matched:
  - Stationary profiles before and after inversion
  - Rigid core acceleration
  - Inversion timescale
  - Transient counter acceleration of the edge

Z_{eff} independence

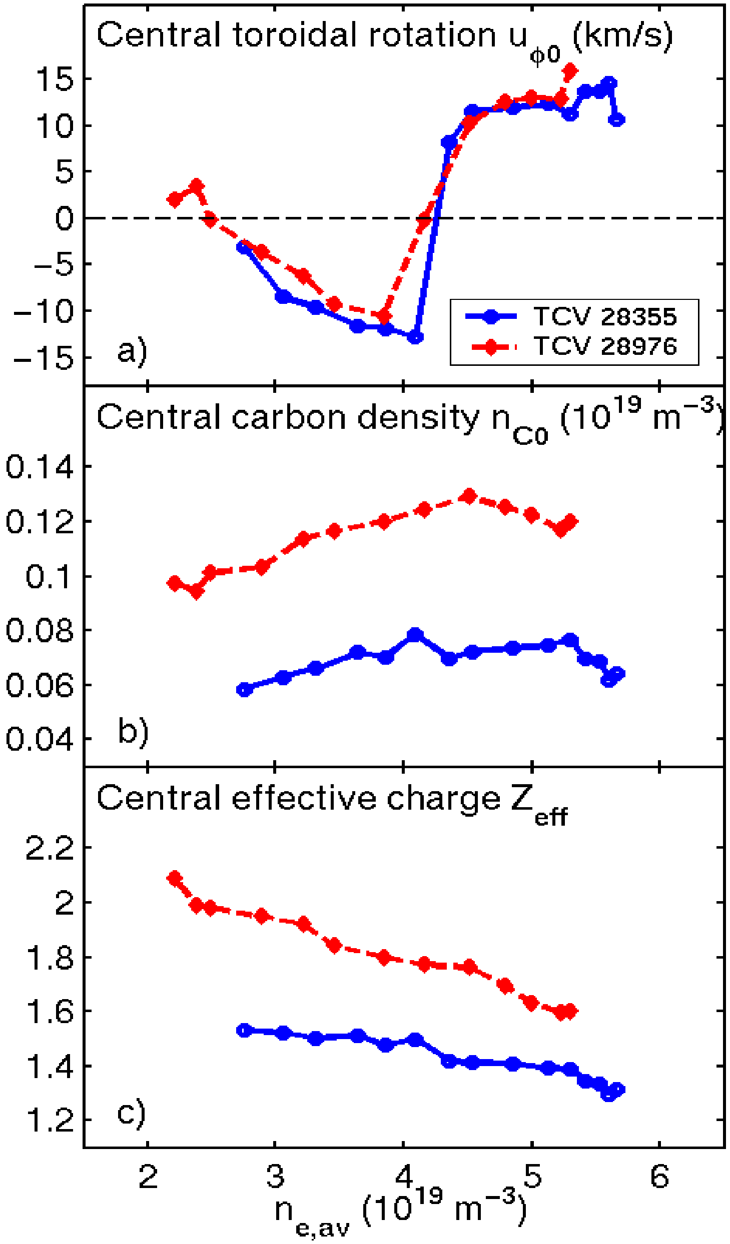

- Two discharges shown where there is large measured difference in the Carbon content (from CXRS)
- Toroidal velocity evolution and the toroidal reversal are very similar

Limited L-mode: u_φ profile across inversion

I_p=320 kA, q_{95} = 2.8 ,δ=0.5, κ=1.6

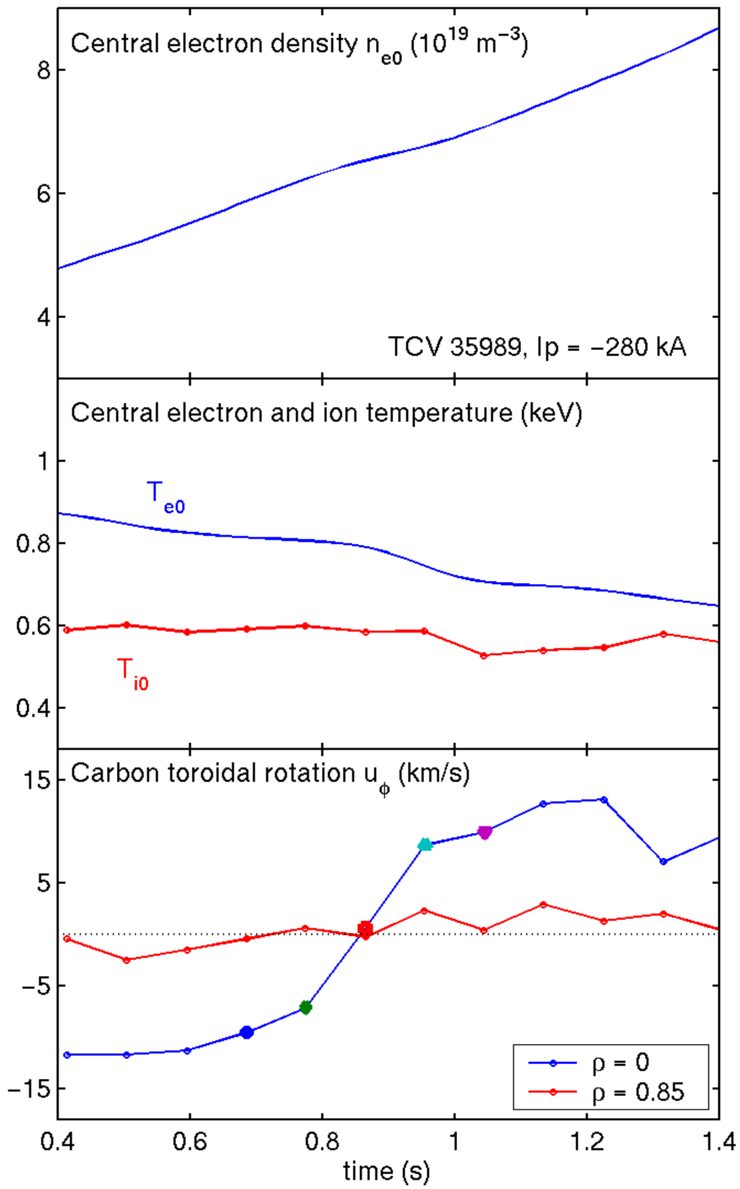

Rotation inversion obtained with a density ramp at I_p=const

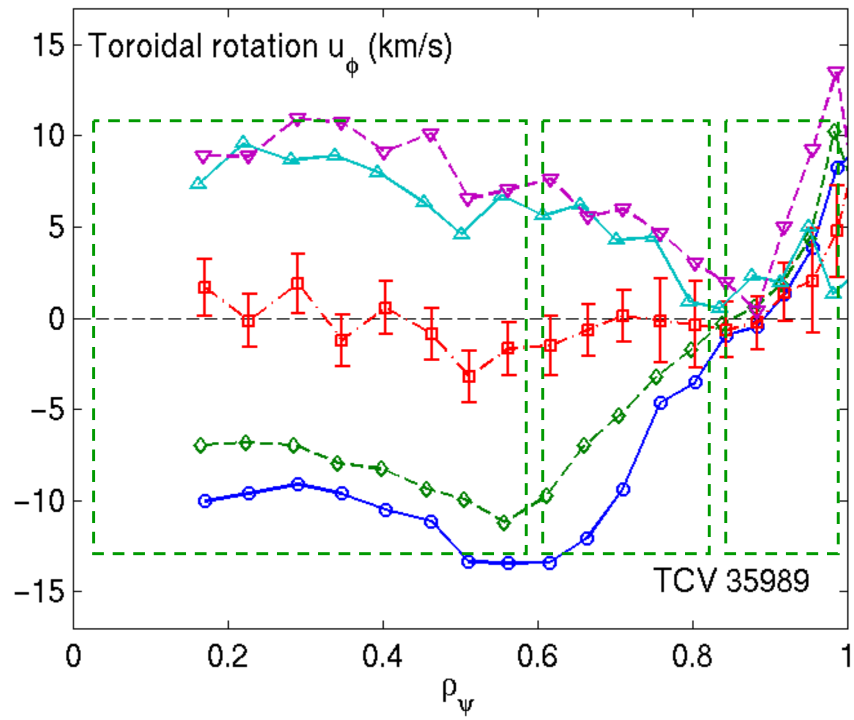

- Core accelerates rigidly
- Transient cnt-acceleration of the edge
- Momentum conservation dynamic followed by edge dissipation

DNBI upgrade

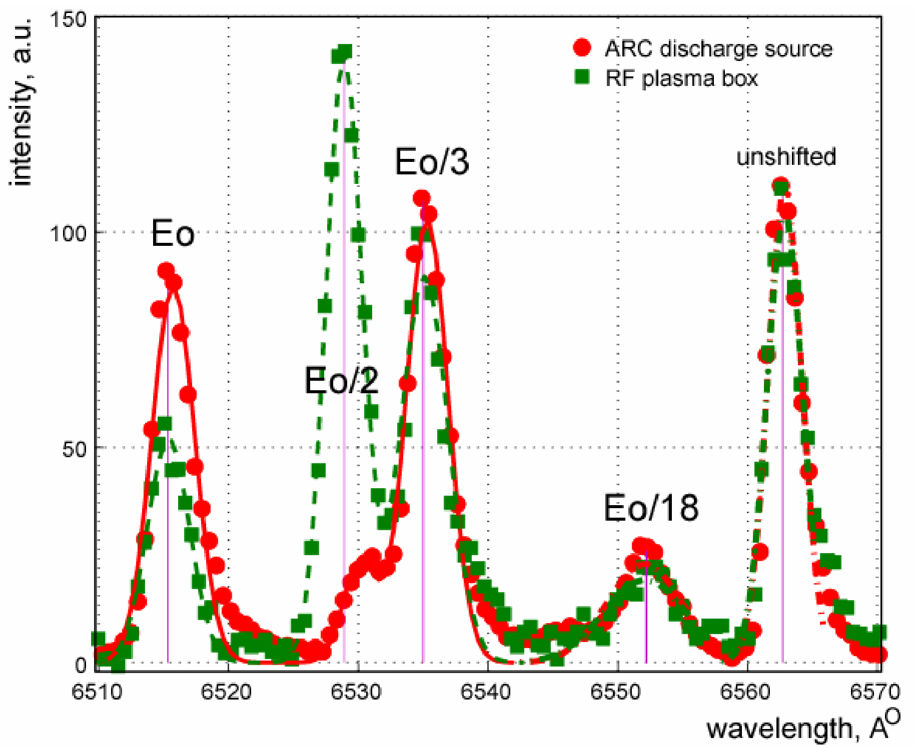

DNBI has been upgraded to improved the performaces without increasing injected power:

1. RF source replaced with arc-discharge source
   full energy (H^+) fraction from 40-60% to 85%
   → **more penetration**

2. New focusing grids :
   divergence reduced from 0.65-0.75° to 0.5°
   → **more CX signal**

<u>Sample frequency 90 → 50 ms</u>

<u>Measurements at higher densities (H-mode)</u>

Triangularity scan: $\delta<0$

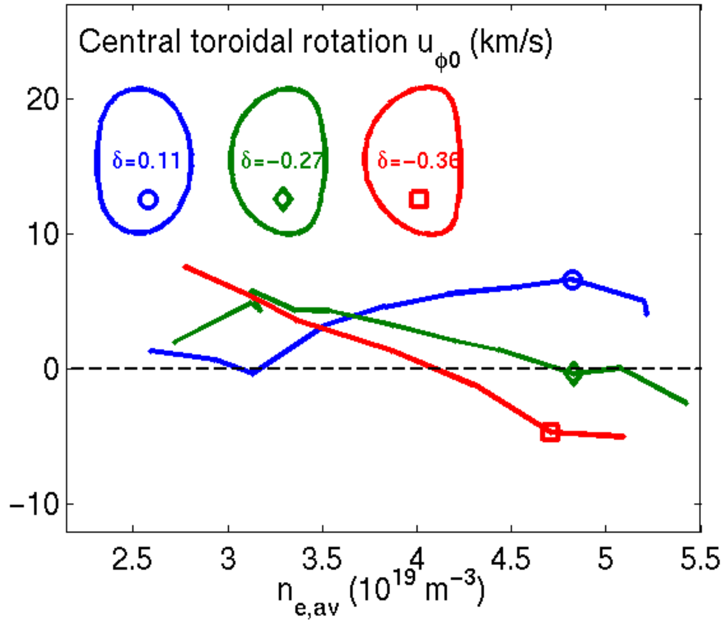

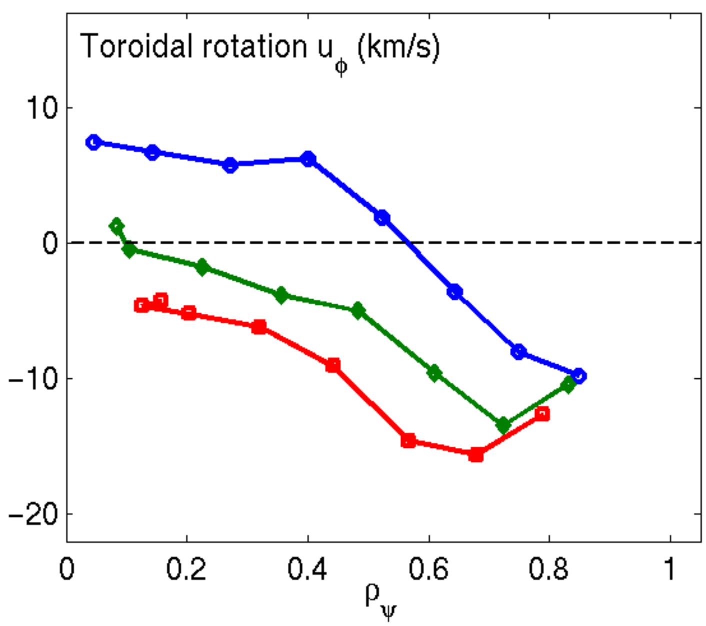

$\delta = 0.11, -0.27, -0.36$

- Toroidal rotation inversion not seen
- Plasma toroidal profile flat in core with stronger counter-current rotation outside
- Profile flattens with decreasing δ with whole profile accelerating in counter-current direction with n_e.
- Confinement increase (*Camenen et al. Nucl. Fusion, **2007**, 47, 510*)

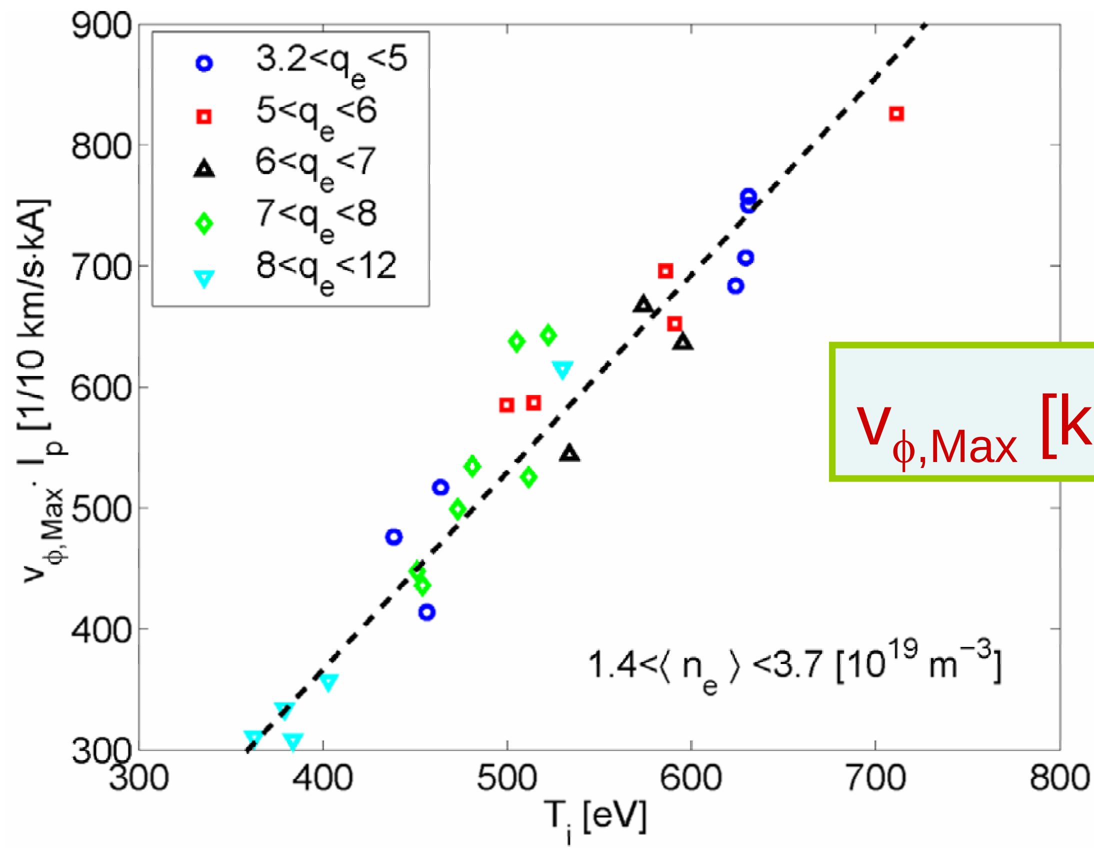

Empirical Scaling Law

$$v_{\phi,Max}\ [km/s] = -12.5\ T_{i,0}\,/I_p\ [eV/kA]$$

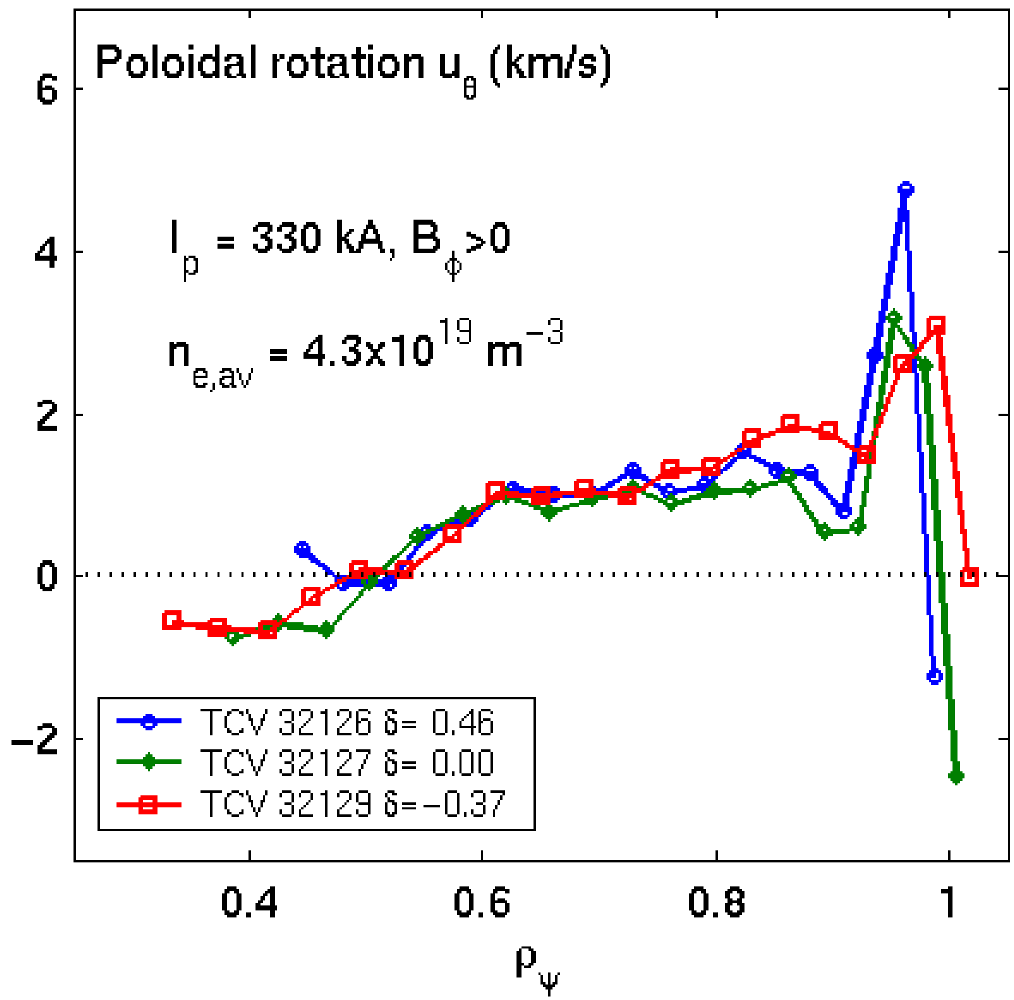
Poloidal rotation u_θ (km/s)
I_p = 330 kA, B_ϕ>0
$n_{e,av}$ = 4.3x10^{19} m^{-3}
TCV 32126 δ= 0.46
TCV 32127 δ= 0.00
TCV 32129 δ=−0.37
6
4
2
0
−2
0.4
0.6
0.8
1
ρ_ψ

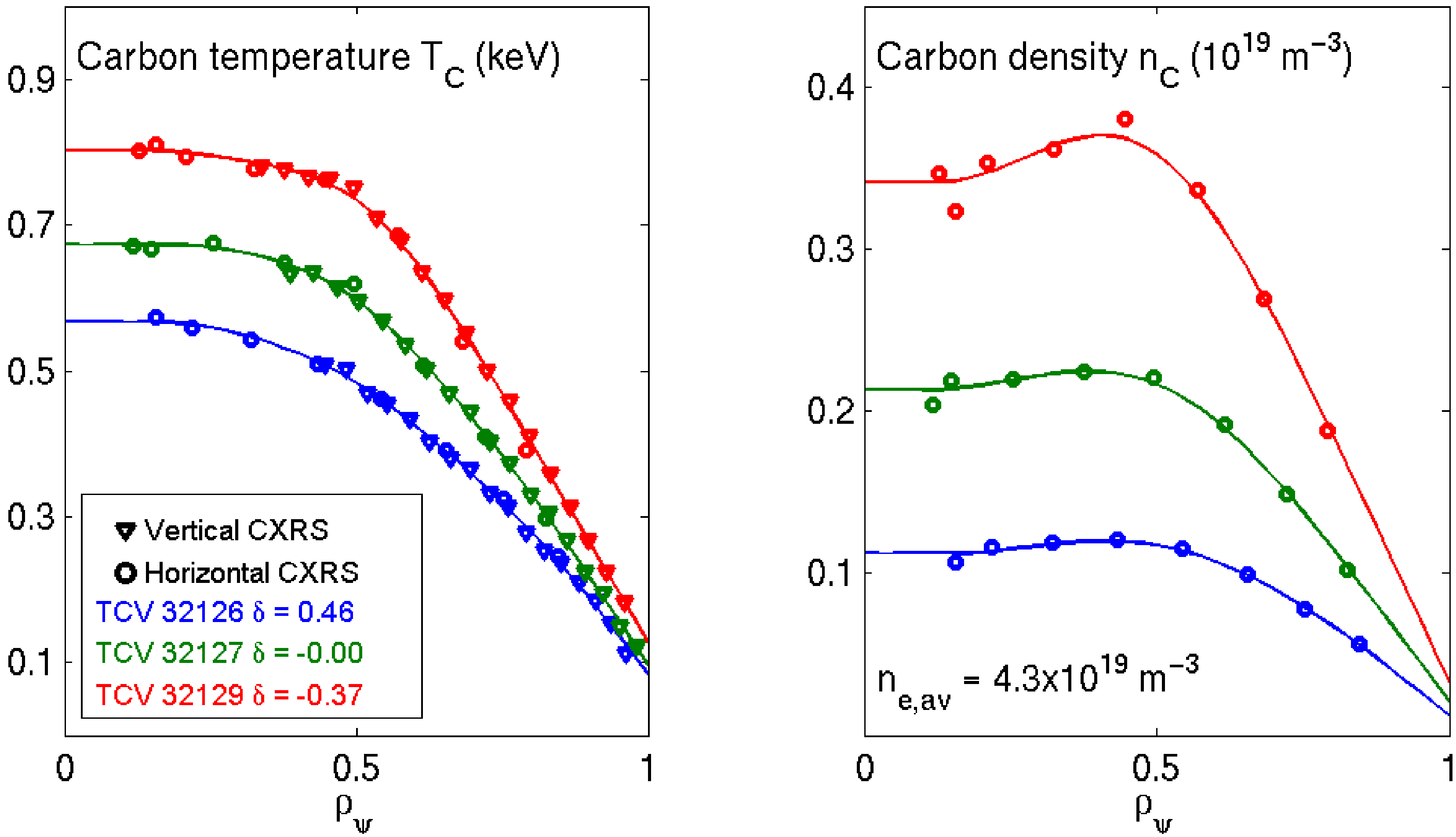
Carbon temperature T_C (keV)
0.9
0.7
0.5
0.3
0.1
0
0.5
1
ρ_ψ
Vertical CXRS
Horizontal CXRS
TCV 32126 δ = 0.46
TCV 32127 δ = -0.00
TCV 32129 δ = -0.37
Carbon density n_C (10^19 m^-3)
0.4
0.3
0.2
0.1
n_e,av = 4.3x10^19 m^-3
0
0.5
1
ρ_ψ

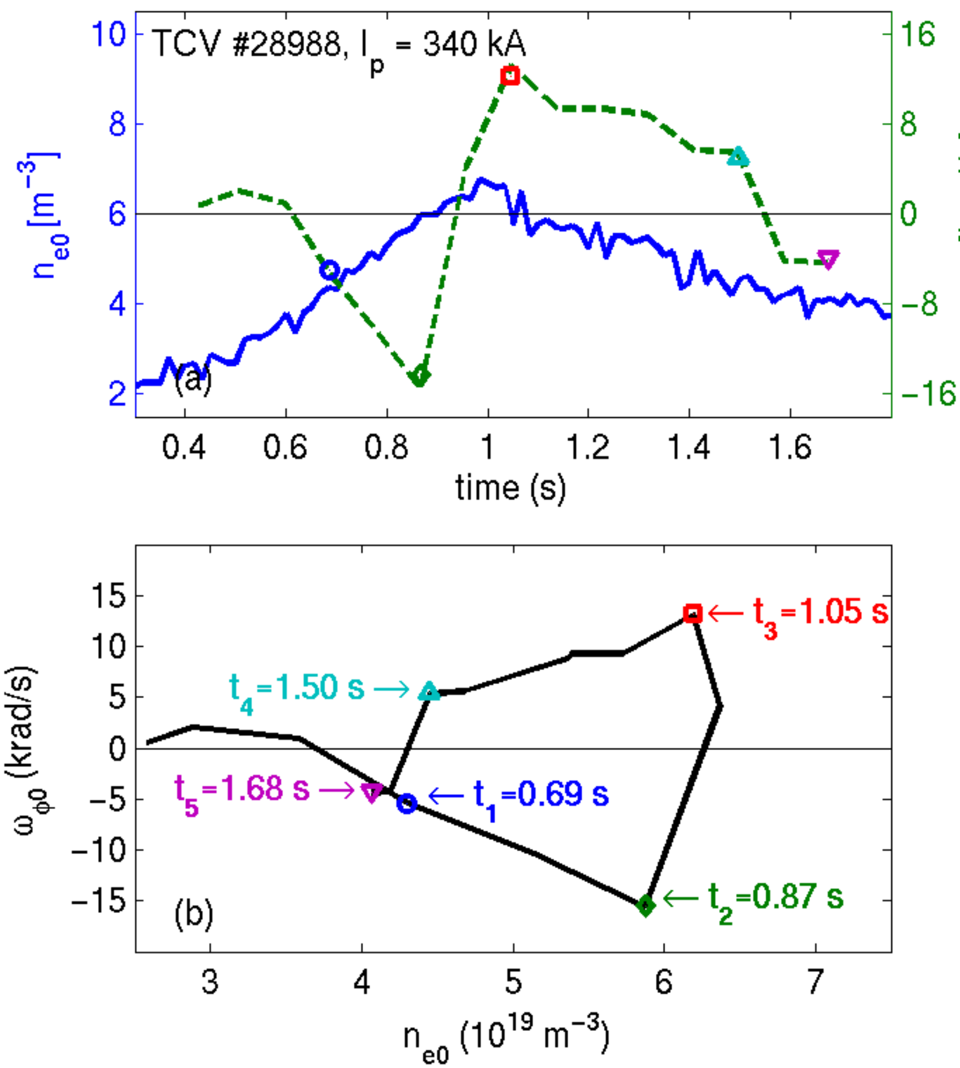
TCV #28988, I_p = 340 kA
n_{e0} [m^{-3}]
$\omega_{\phi 0}$ [krad/s]
time (s)
(a)
t_3=1.05 s
t_4=1.50 s
t_5=1.68 s
t_1=0.69 s
t_2=0.87 s
$\omega_{\phi 0}$ (krad/s)
n_{e0} (10^{19} m^{-3})
(b)

X2 induced back transition

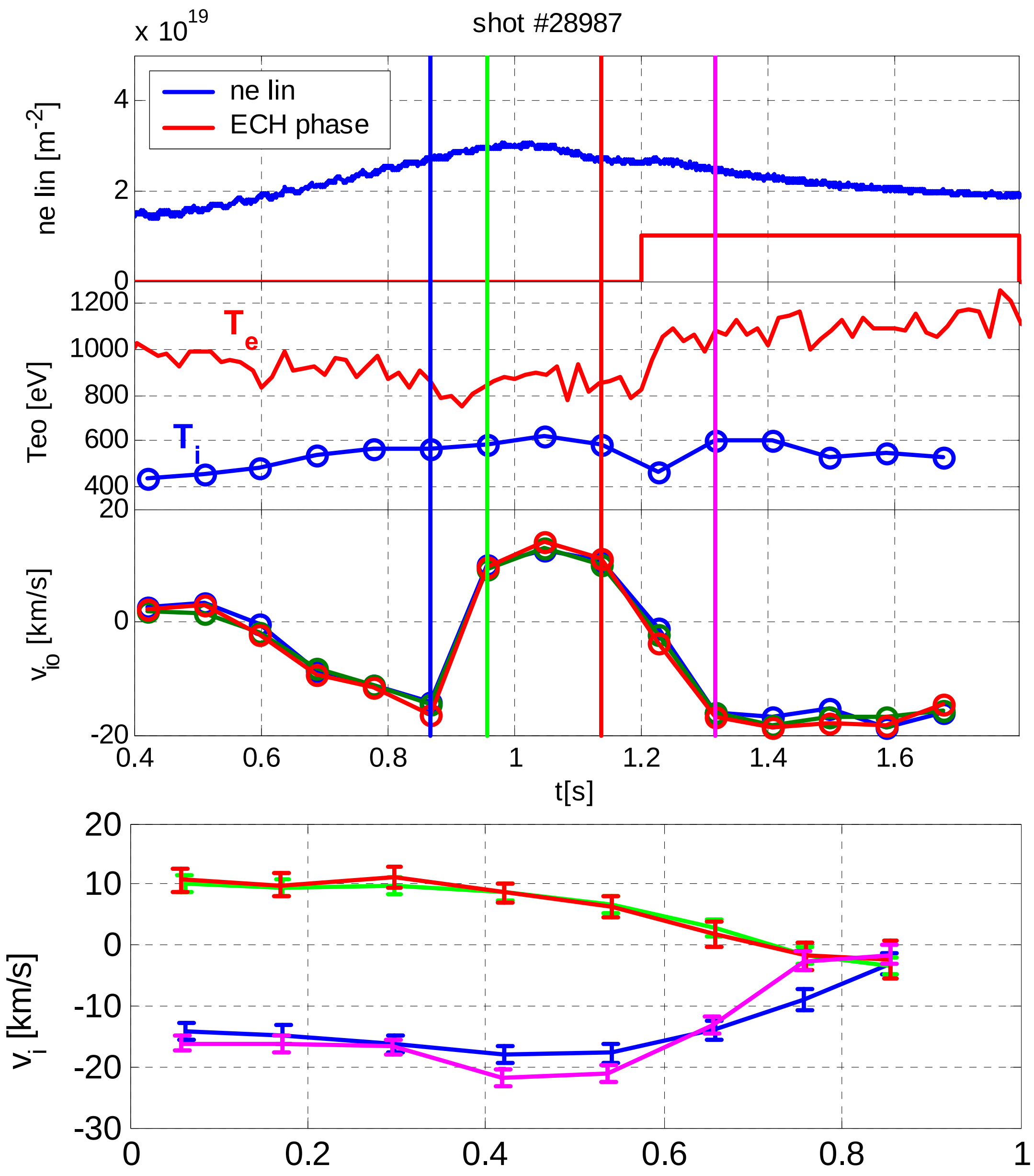

ECH heating -> higher threshold

ECH heating can drive a back inversion. Done!

- ne threshold is comparable
- pre-inversion velocity profiles are recovered

X3 induced transition

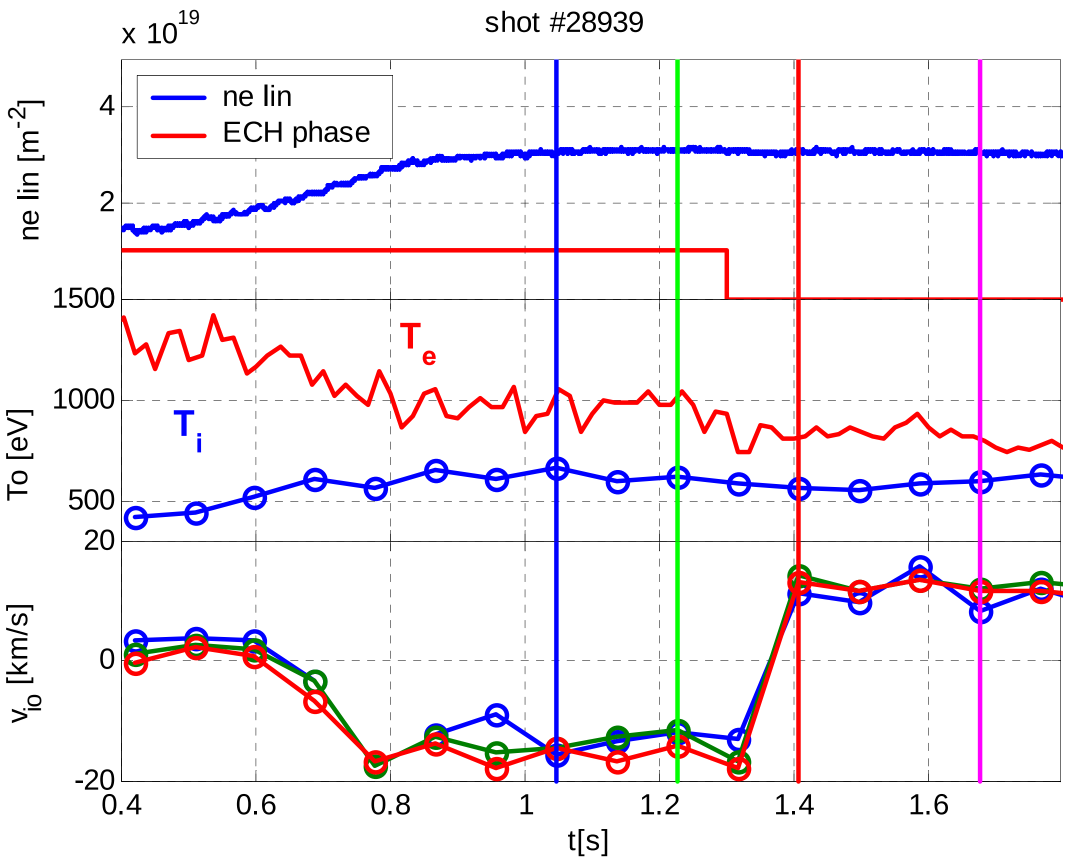

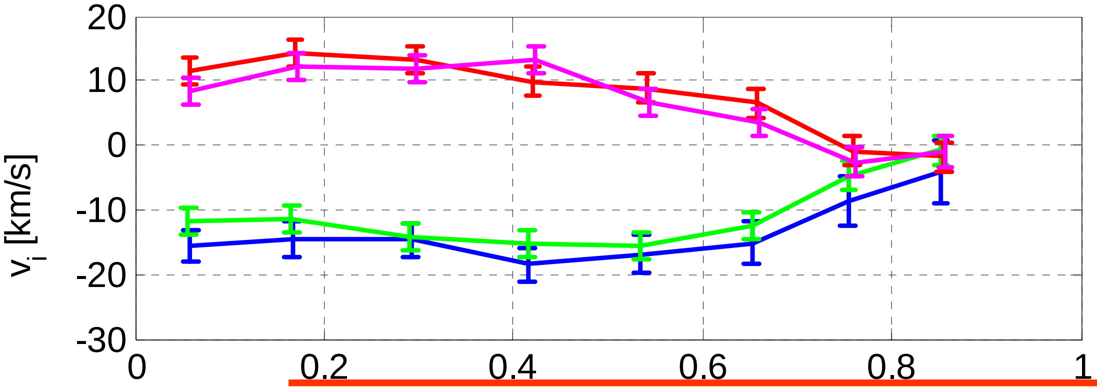

ECH heating -> higher threshold

Removing ECH heating we can drive a *direct* inversion. Done!

In this case n_e profile is constant!

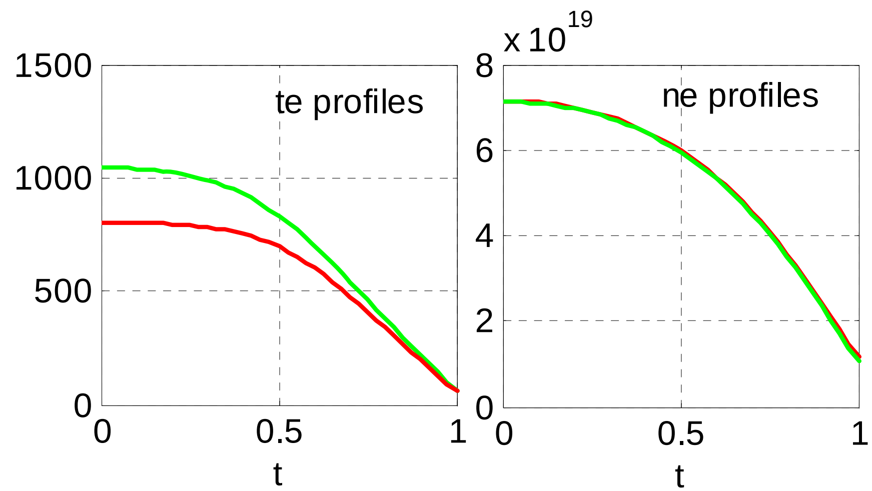

n_e is not the main driving quantity